

Modeling Structure and Country-specific Heterogeneity in Misclassification Matrices of Verbal Autopsy-based Cause of Death Classifiers

Sandipan Pramanik¹, Scott Zeger¹, Dianna Blau², and Abhirup Datta^{*1}

¹Department of Biostatistics, Johns Hopkins University

²Global Health Center, US Centers for Disease Control and Prevention

December 7, 2023

Abstract

Verbal autopsy (VA) algorithms are routinely used to determine individual-level *causes of death (COD)* in many low-and-middle-income countries, which are then aggregated to derive population-level *cause-specific mortality fractions (CSMF)*, essential to informing public health policies. However, VA algorithms frequently misclassify COD and introduce *bias* in CSMF estimates. A recent method, *VA-calibration*, can correct for this bias using a VA misclassification matrix estimated from paired data on COD from both VA and *minimally invasive tissue sampling (MITS)* from the *Child Health and Mortality Prevention Surveillance (CHAMPS) Network*. Due to the limited sample size, CHAMPS data are pooled across all countries, implicitly assuming that the misclassification rates are homogeneous.

In this research, we show that the VA misclassification matrices are substantially heterogeneous across countries, thereby biasing the VA-calibration. We develop a coherent framework for modeling country-specific misclassification matrices in data-scarce settings. We first introduce a novel *base model* based on two latent mechanisms – *intrinsic accuracy* and *systematic preference* to parsimoniously characterize misclassifications. We prove that they are identifiable from the data and manifest as a form of invariance in certain misclassification odds, a pattern evident in the CHAMPS data. Then we expand from this base model, adding higher complexity and country-specific heterogeneity via interpretable *effect sizes*. *Shrinkage priors* balance the *bias-variance tradeoff* by adaptively favoring simpler models. We publish uncertainty-quantified estimates of VA misclassification rates

*Email address for correspondence: abhidatta@jhu.edu

for 6 countries. This effort broadens VA-calibration’s future applicability and strengthens ongoing efforts of using VA for mortality surveillance.

Keywords: Bayesian, hierarchical modeling, verbal autopsy, minimally invasive tissue sampling, global health.

1 Introduction

Understanding a population’s burden of diseases is essential to effective public health practice. This heavily relies on *cause-specific mortality fractions (CSMF)* that measure the prevalence of different diseases by aggregating individual-level *causes of death (COD)* data. However, complete and accurate COD information from a *complete diagnostic autopsy (CDA)* is uncommon in many *low and middle-income countries (LMICs)* (Nichols et al., 2018). Therefore, alternative approaches like *minimally invasive tissue sampling (MITS)* and *verbal autopsy (VA)* are being increasingly relied upon. For COD determination, MITS is highly accurate relative to *full diagnostic autopsies* (Bassat et al., 2017; Menendez et al., 2017). However, due to its resource-intensive nature, it is predominantly conducted in select hospitals and is therefore not *scalable* to an entire population.

VA is a non-invasive procedure that systematically interviews household members and gathers a decedent’s health history and symptoms (Mikkelsen et al., 2015; Wang et al., 2017; Adair and Lopez, 2018). The interview responses are then input into a *computer-coded VA (CCVA) algorithms* (referred to here as VA algorithm) to assign a COD. Given the scalability afforded by automation, VA has emerged as the predominant source for determining COD in community settings and is routinely used to estimate CSMF (de Savigny et al., 2017; Garenne, 2014; Soleman et al., 2006; Setel et al., 2005). *Countrywide Mortality Surveillance for Action (COMSA)* programs have recently demonstrated this where nationwide VA studies were conducted in Mozambique (COMSA-Mz) and Sierra Leone to generate mortality rates and COD data for all ages to monitor the Sustainable Development Goals for health (Fiksel et al., 2023; Gilbert et al., 2023; Macicame et al., 2023; Carshon-Marsh et al., 2022).

While VA is the only feasible tool for mortality surveillance at national scales, VA-predicted causes of death (VA-COD) suffer from substantial *misclassification bias* when compared to MITS or physician’s diagnosis (Clark et al., 2018; Adair and Lopez, 2018; Datta et al., 2020; Fiksel et al., 2022). A naive aggregation of VA-COD inherits this bias and produces highly inaccurate CSMF estimates. Recent research has introduced *VA-calibration* to rectify this anticipated bias (Datta et al., 2020; Fiksel et al., 2022, 2023). VA-calibration utilizes a limited set of paired CODs predicted from both VA and a standard reference diagnosis, such as MITS, to understand the misclassification rates of VA algorithms. For C causes of death, the *misclassification matrix* (also referred to as the *confusion matrix*) is a $C \times C$ matrix whose $(i, j)^{th}$ entry is the *conditional probability* that the VA algorithm predicts cause j given the true (or reference) cause i . Thus, its diagonal elements are *sensitivities* and off-diagonal entries are *false positive*

rates. In a *hierarchical Bayesian setup*, VA-calibration uses this matrix to *calibrate* the raw estimates and it has been shown to significantly enhance the CSMF estimation accuracy.

Recently, VA-calibration was used to produce CSMF estimates for neonatal and children (1–59 months) deaths at the national level in Mozambique (Fiksel et al., 2023; Gilbert et al., 2023; Macicame et al., 2023). Utilizing data collected in the *Child Health and Mortality Prevention Surveillance (CHAMPS) project*, this study presents misclassification rate estimates of VA compared to MITS. CHAMPS records paired CODs predicted from both VA and MITS and currently spans six countries, including Mozambique. In order to enhance the sample size and *precision* of estimates, the analysis *pooled* CHAMPS data from all countries rather than solely relying on the data collected in Mozambique.

The misclassification matrix is the cornerstone of VA-calibration and it is crucial to ensure the validity of its estimation. Pooling data from all countries implicitly makes a *homogeneity assumption* that misclassification rates are the same for all countries. In the context of VA-calibration, this represents a *bias-variance tradeoff*. Thus any possible gains in precision from pooling the data are offset by possible bias introduced if data from other countries are not representative of Mozambique or other target countries.

There are two statistical challenges in the estimation of VA misclassification matrices. First, in Figure 1 we demonstrate that the observed misclassification proportions vary significantly across countries. The presence of *country-specific heterogeneity* contradicts the assumption of homogeneity that was previously used to justify a pooled misclassification matrix. Consequently, the pooled estimates can introduce bias in the resulting CSMF estimates. Second, while it would be preferable to estimate VA-misclassification rates separately for each country to accommodate heterogeneity, the limited number of observed MITS cases per country presents a challenge, with 6 or fewer samples for 75% of the cells in the matrix and 32% of the cells have zero samples (See Figure S1 in the supplement). Although this could potentially reduce bias (improve accuracy), the insufficient sample size would increase *uncertainty* (reduce precision). This is undesirable for subsequent calibration and would also preclude extrapolation to countries that are not among the CHAMPS sites.

In this article, we propose a framework for modeling heterogeneity in VA misclassification matrices across countries with three key contributions that balance the bias-variance tradeoff. First, we introduce a novel and parsimonious *base model* for misclassification matrices that assumes a lower-dimensional structure based upon two novel mechanisms for correct or mis-classification – *intrinsic accuracy* of a classifier to correctly identify the true cause, and the *systematic preference (or pull)* of the classifier towards predicting a cause regardless of what the true cause is. We show that these mechanisms, if present, can be identified based on observed misclassification counts of a classifier (See Theorem 3.1). Figure 3 shows that both mechanisms are present for *Insilico VA*, the leading VA algorithm. The mechanisms borrow information across matrix cells leading to considerable dimension reduction, which is particularly advantageous in data-scarce settings.

The second contribution builds upon the parsimonious base model and proposes a nested hierarchical model for country-specific misclassification matrices with increasing complexity. This introduces a broader class of distributions on country-specific misclassification matrices that shrinks towards the base model. Each hierarchy promotes shrinkage towards the lesser complex model through three effect size parameters that explicitly control the *pull strength* (informing on the degree of diversion from the base model) and the *degree of heterogeneity*. We assume *shrinkage priors* on them to promote *continuous shrinkage*. In the absence of compelling evidence supporting complexity, the nested structure adaptively favors simpler models, enhancing the precision of estimates when dealing with limited sample sizes. We assessed the framework through extensive simulation studies and applied it to generate misclassification rates for InSilicoVA in six countries – Bangladesh, Ethiopia, Kenya, Mali, Mozambique, and Sierra Leone. The estimates will be used to calibrate VA data for the next set of regional and national under-5 cause-specific mortality estimates for the Sustainable Development Goals (Perin et al., 2022).

The rest of the article is organized as follows. We describe the motivating dataset in Section 2. In Section 3 we propose the methodology. Section 4 investigates its empirical properties through extensive simulation studies depicting the real-life application. We revisit the motivating dataset in Section 5 and apply the proposed framework to obtain the misclassification matrix estimate for *InSilicoVA*, a widely used VA algorithm. We conclude in Section 6 with a discussion of findings and future research opportunities.

2 Motivating Dataset From The *CHAMPS Network*

The Child Health and Mortality Prevention Surveillance (CHAMPS) is an ongoing initiative dedicated to comprehensive child mortality surveillance in multiple countries (Blau et al., 2019; Salzberg et al., 2019). For a limited number of deaths among neonates, children aged 1-59 months, and stillbirths in hospital facilities, CHAMPS performs *minimally invasive tissue sampling (MITS)* to obtain a comprehensive COD diagnosis. With VA-predicted CODs also recorded for the deaths, this generates a labeled dataset of paired MITS- and VA-CODs across multiple sites in South Asia and Africa. This constitutes a unique resource for assessing the algorithmic precision of VA in estimating mortality rates.

The previous analysis of pooled CHAMPS COD data using VA-calibration unveiled substantial misclassification rates across age groups for various VA algorithms (Fiksel et al., 2023; Gilbert et al., 2023). Subsequently, CSMF estimates for neonates and children aged 1-59 months were obtained in Mozambique by calibrating VA-only data from COMSA-Mz. Pooling of CHAMPS data across all the countries implicitly makes the assumption that the misclassification rates are homogeneous, and was done in Fiksel et al. (2023) to increase sample size and precision of the misclassification matrix estimate. With more data being collected, one can assess for heterogeneity in the misclassification rates across countries.

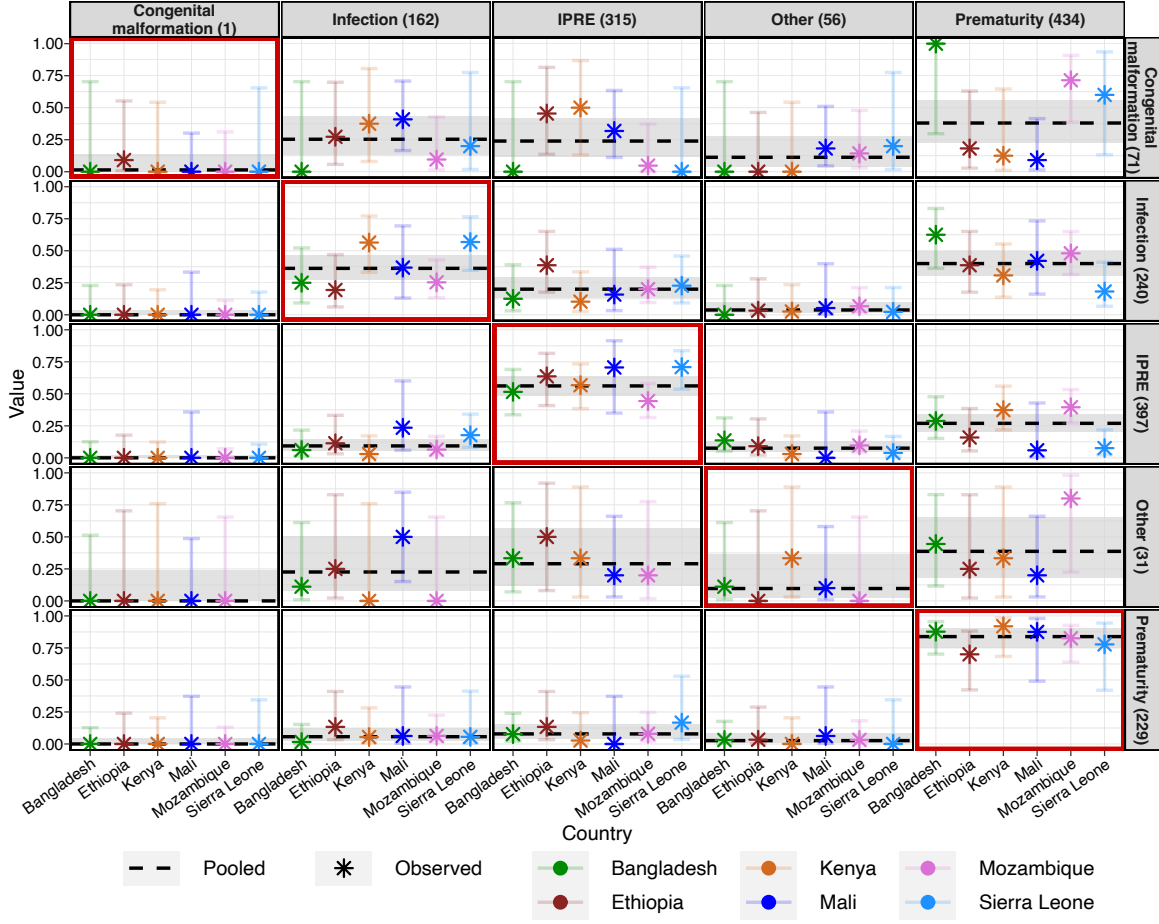


Figure 1: Country-specific empirical misclassification matrices of InSilicoVA concerning MITS for neonatal deaths in the CHAMPS dataset. Rows and columns are MITS and VA-predicted causes. The diagonal and off-diagonal panels respectively display the sensitivities and false positives. The dashed black horizontal lines are average rates, *pooled* across countries. The error bars and grey bands are 95% confidence intervals (obtained using `MultinomCI()` in R package `DescTools`). Numbers in parentheses denote the sample size.

In Figure 1, we analyze the misclassification pattern for InSilicoVA using 570 neonatal deaths that occurred within CHAMPS network hospitals in Bangladesh, Ethiopia, Kenya, Mali, Mozambique, and Sierra Leone between July 2017 and 2023. Following Fiksel et al. (2023), both VA and MITS-COD are aggregated into $C = 5$ broad categories: *congenital malformation*, *infection*, *intrapartum related events (IPRE)*, *prematurity*, and *other*.

The Figure displays observed misclassification proportions in each country together with the pooled proportion (dashed black line). The figure highlights two main challenges.

- **Heterogeneity across countries.** Compared to the pooled values, the country-

specific proportions substantially deviate across countries for several MITS-VA cause pairs, indicating a significant variation in InSilicoVA’s misclassification between countries. This is particularly pronounced for sensitivities of infection and IPRE, and false positive proportions for MITS-VA cause pairs congenital malformation-IPRE and infection-prematurity. Given the current implementation of VA-calibration is based on the homogeneity assumption, this would produce locally incongruous misclassification rate estimates and could adversely affect the accuracy of calibrated CSMF estimates.

- **Limited size of CHAMPS data.** In the presence of a strong heterogeneity as in Figure 1, implementing VA-calibration separately for each country can enhance estimation accuracy. However, the number of CHAMPS cases is quite limited in some countries. The CHAMPS dataset used here has a total of 570 cases across 6 countries for a 5×5 misclassification matrix, which leaves less than 4 cases per cell on average. Combined across countries, 6 or fewer samples are observed for 75% of the MITS-VA cause pairs, while 32% are unobserved (See Figure S1 in the supplement). This is grossly inadequate for unstructured estimation of C^2 misclassification rates in each country separately. Such estimates will be highly imprecise, rendering them practically futile for any subsequent calibration of VA-only data.

3 Method

In this section, we propose a comprehensive framework to mitigate the above issues. First, we propose a novel parsimonious model for estimating a homogeneous misclassification matrix for a classifier in a very low sample size setting. We then generalize to a nested modeling framework of progressively richer parameterized models by relaxing the parsimony and incorporating country-specific heterogeneity through adaptive shrinkage.

3.1 Base Model Based On *Intrinsic Accuracy* And *Systematic Preference*

Let $\Phi = (\phi_{ij})$ denote the $C \times C$ misclassification matrix of COD predictions from a VA classifier (V) with respect to the MITS COD diagnosis (M). The diagonal $\phi_{ii} = \mathbb{P}(V = i | M = i)$ is the sensitivity for cause i , and for $i \neq j$, the off-diagonal $\phi_{ij} = \mathbb{P}(V = j | M = i)$ is the false positive (FP). So Φ is a Markov matrix (i.e., non-negative entries and rows add up to one). Due to the limited availability of MITS cases and the prevalence of unrecorded MITS-VA cause pairs, separately estimating the C^2 misclassification rates of Φ in an unstructured manner is undesirable, especially when extending to country-specific estimates. We propose a novel and parsimonious base model recognizing two fundamental processes for a classifier – algorithm’s design in correctly identifying a MITS cause, and the systematic preference that inclines it towards favoring certain causes.

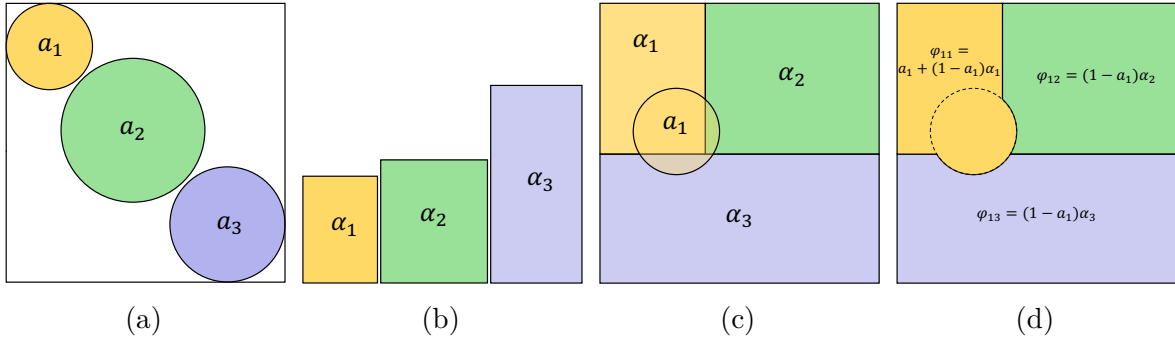


Figure 2: For 3 causes, (a) and (b) show intrinsic accuracy and pull as diagonal and column effects. The Venn diagrams in (c) and (d) collectively illustrate the mechanism that defines sensitivity and false positives in the base model for MITS cause 1. A similar mechanism applies to other MITS causes. Causes are coded in different colors.

Intrinsic Accuracy (Diagonal Effect). Given VA algorithms are designed to produce correct matches, let a_i denote its *intrinsic accuracy* for cause i , indicating the probability that the algorithm correctly identifies cause i by design. Conceptually, intrinsic accuracy from predicting cause i originates through a specific combination of symptoms reported in the VA record, which manifest only when the true cause is i .

Systematic Preference or Pull (Column Effect). In scenarios where an algorithm fails to produce a correct match by design, our base model assumes a simplistic scenario where it assigns any of the C causes with prespecified probabilities regardless of what the true (MITS) cause is. This can be interpreted as the algorithm’s *systematic preference or pull* towards predicting a cause. For cause j we denote the pull by α_j , and it is the probability of assigning cause j in failing to match the correct cause i by design.

Intrinsic accuracy and pull encapsulate key algorithmic characteristics and govern the misclassification mechanism. Although we do not witness the mechanisms directly, the observed misclassification proportions are a combined influence of these fundamental events. The intrinsic accuracies a_i are *diagonal effects* and they model correct matches by design, adding to the diagonal entries of Φ . The pulls α_j ’s, on the other hand, are *column effects* as they specify probabilities of adding to the columns of Φ regardless of the row (MITS cause).

The mechanism is formally depicted in Figure 2. A correct match for true cause i occurs either by design (with probability a_i), or by the pull α_i towards cause i in failing to match by design (with probability $(1 - a_i)\alpha_i$). For the same true cause, a misclassification into cause j occurs only by the pull α_j towards cause j after it fails to match by design (with probability $(1 - a_i)\alpha_j$). So for $a_i \in [0, 1]$, $\alpha_j \in [0, 1]$, and $\sum_{j=1}^C \alpha_j = 1$ we have:

$$\begin{aligned} \phi_{ii} &= a_i + (1 - a_i)\alpha_i \quad \forall i, \\ \phi_{ij} &= (1 - a_i)\alpha_j \quad \forall i, j \neq i. \end{aligned} \tag{1}$$

The base model offers numerous benefits in efficiently modeling the misclassification matrix. It posits a parsimonious characterization of misclassifications, requiring estimation of only $2C - 1$ parameters (C many a_i 's and $C - 1$ many α_j 's). This accrues considerable dimension-reduction contrasted with the unstructured model which has $C^2 - C$ free parameters. This parsimony will later allow extension to modeling country-specific variations using very limited sample sizes. Additionally, introduction of the systematic preference enables us to explicitly measure the error that the algorithm systematically incurs (See Figure 10a). Beyond calibrating for the implied misclassification rates, it also allows us to identify causes that a VA algorithm systematically favors, providing deeper insights into its functioning and opening up opportunities for designing more precise VA algorithms.

Intrinsic accuracy and systematic preference are hypothesized latent mechanisms for misclassification. They cannot be directly inferred from the data as we only observe overall misclassification counts for each VA-MITS cause pair. Below we provide a theoretical justification for positing the base model. All proofs are in the supplement.

Theorem 3.1 (Characterization of base model in terms of constant odds) *The misclassification matrix Φ can be completely specified using intrinsic accuracy and systematic preference as in (1) if and only if the misclassification odds ϕ_{ij}/ϕ_{ik} of VA predicting cause j or k is constant with respect to the MITS cause i for any $i \neq j, k$.*

The Theorem states that the base model (1) can be equivalently characterized as

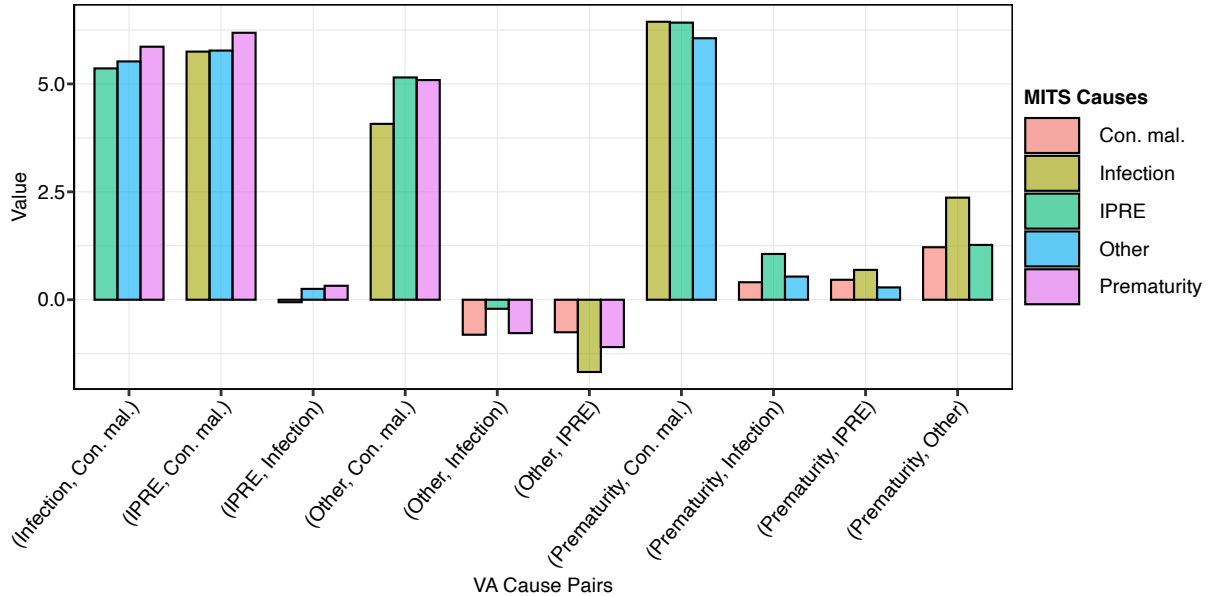


Figure 3: Similarity of misclassification log odds $\log(\phi_{ij}/\phi_{ik})$ between MITS causes for all VA cause pairs. The horizontal axis shows VA cause pairs (j, k) . For each cause pair, the grouped bar plot presents log odds for all MITS causes $i \neq j, k$. Con. mal. denotes Congenital malformation.

the odds of the VA algorithm misclassifying an MITS cause into cause j or k , where the odds are only a function of (j, k) and do not depend on the MITS cause. This provides an equivalence between the base model and misclassification odds that can be directly estimated from the observed misclassification counts. Figure 3 plots the log-odds for the neonatal CHAMPS data from InSilicoVA. We see a strong pattern — for each pair (j, k) of VA causes the odds ϕ_{ij}/ϕ_{ik} are relatively constant across different MITS causes i . Figure 3 combined with the characterization in Theorem 3.1 suggests strong evidence in favor of the base model.

The next result proves that given only observed data on the misclassification counts, the parameters specifying intrinsic accuracy and systematic preference can be identified. Let $\{(V_r, M_r)\}_{r \in s}$ denote the paired VA- and MITS-COD for CHAMPS cases in site (country) s . Let us define the observed misclassification count matrix in country s as

$$\mathbf{T}_s = (t_{sij}) = \sum_{r \in s} \mathbb{I}(V_r = j \mid M_r = i), \quad (2)$$

and the pooled misclassification matrix $\mathbf{T} = \sum_{s=1}^S \mathbf{T}_s$. Let $n_{si} = \sum_{r \in s} \mathbb{I}(M_r = i)$ denote the number of cases in country s with MITS cause i and $n_i = \sum_{s=1}^S n_{si}$ is the total sample size for MITS cause i across all CHAMPS sites. Let $\mathbf{T}_{i*} = (t_{i1}, \dots, t_{iC})^T$ and $\Phi_{i*} = (\phi_{i1}, \dots, \phi_{iC})^T$ denote the i^{th} row of \mathbf{T} and Φ . Then we can model the observed misclassification counts as

$$\mathbf{T}_{i*} \stackrel{ind}{\sim} \text{Multinomial}(n_i, \Phi_{i*}), \quad \forall i = 1, \dots, C. \quad (3)$$

Proposition 3.1 (Identifiability of base model) *Under the base model (1) for the misclassification rate matrix, the likelihood (3) is identifiable with respect to the a_i 's and α_j 's.*

The proposition confirms that under the base model, we can uniquely recover intrinsic accuracies and pull that govern the misclassification mechanism. The result validates the base model and implies that the accuracy and pull estimates will be asymptotically consistent. We do not pursue a formal proof of consistency as the sample size is very low.

3.2 A General Homogeneous Model

Despite the evidence in Figure (3) for InSilicoVA's misclassification among neonatal deaths in CHAMPS, it might be too restrictive in practice to assume that misclassification rates exactly satisfy the base model (1). Also, the extent to which misclassification rates satisfy this structure may vary across age groups and choice of VA algorithms. Instead, we propose a more general model that shrinks towards the base model to achieve parsimony.

First, we decompose the false positive rates as

$$\phi_{ij} = (1 - \phi_{ii}) q_{ij} \quad \forall i \neq j, \quad (4)$$

where ϕ_{ii} is the sensitivity and $q_{ij} = \mathbb{P}(V = j | M = i, V \neq i)$ is defined as the *relative false positive (relative FP)*. Note that, under base model (1), we have

$$q_{ij} = \frac{\mathbb{P}(V = j, M = i)}{\sum_{k \neq i} \mathbb{P}(V = k, M = i)} = \frac{(1 - a_i)\alpha_j}{(1 - a_i)\sum_{k \neq i} \alpha_k} = \frac{\alpha_j}{1 - \alpha_i} := \alpha_{ij}^*. \quad (5)$$

We propose probabilistic models for both sensitivities and relative FP, and shrink them towards respective expressions in the base model. The complete Bayesian hierarchical model for modeling a general homogeneous misclassification matrix is given by

$$\begin{aligned} \mathbf{T}_{i*} &\stackrel{ind}{\sim} \text{Multinomial}(\Phi_{i*}), \text{ with } \phi_{ij} = (1 - \phi_{ii})q_{ij} \quad \forall i \neq j, \\ \phi_{ii} &\stackrel{ind}{\sim} \text{Beta}(0.5 + \kappa(a_i + (1 - a_i)\alpha_i), 0.5 + \kappa(1 - a_i)(1 - \alpha_i)) \text{ with } \kappa > 0, \\ \mathbf{q}_{i*} &\stackrel{ind}{\sim} \text{Dir}(0.5 + \lambda \alpha_{i*}^*) \text{ with } \lambda > 0, \\ a_i &\stackrel{iid}{\sim} \text{Beta}(b, d) \text{ with } b, d > 0, \\ \boldsymbol{\alpha} &\sim \text{Dir}(\mathbf{e}) \text{ with } e_1, \dots, e_C > 0. \end{aligned} \quad (6)$$

where $\alpha_{i*}^* = (\alpha_{i1}^*, \dots, \alpha_{i,i-1}^*, \alpha_{i,i+1}^*, \dots, \alpha_{iC}^*)^T$ with α_{ij}^* defined in (5).

This model for the pooled data assigns a Beta prior on the sensitivities ϕ_{ii} and a Dirichlet prior on the relative FP q_{ij} each centered around their respective base models. This ensures that the resulting prior for Φ assigns positive mass to every interior point of the class of $C \times C$ Markov matrices, and given enough data, the posterior will concentrate around the true misclassification matrix. However, in settings with limited data, the choice of a structured prior is important. If $\kappa \uparrow \infty$ and $\lambda \uparrow \infty$ in (6), the model for Φ degenerates exactly to the base model. On the other extreme, as $\lambda, \kappa \downarrow 0$ the priors respectively converge to *Jeffreys non-informative priors* $\text{Beta}(0.5, 0.5)$ and $\text{Dir}(0.5, \dots, 0.5)$ that are often utilized for unstructured modeling of proportions. Thus the addition of just two additional parameters, κ and λ , introduces flexibility into the framework producing a wide spectrum of models with varying degrees of structure.

3.3 Country-specific Misclassification Model

Figure 1 suggests that the misclassification rates of VA with respect to MITS can substantially vary across countries for some cause-pairs. However, due to the limited availability of CHAMPS data per country, it is not feasible to perform a separate unstructured estimation of misclassification rates for each country. Thus a pooled estimation of misclassification rates under a homogeneous model, though not ideal, was previously resorted to as the only viable approach. In this regard, the base model has been designed to address the challenges posed by limited sample sizes by leveraging any discernible structure in the matrix. This significantly reduces the model's dimensionality, allowing us to introduce heterogeneity and generate country-specific estimates for misclassification rates.

Let $\Phi_s = (\phi_{sij})$ denote the misclassification matrix for country s and \mathbf{T}_s is defined as in (2). We propose a heterogeneous model by introducing country-specific probabilistic

models for sensitivities and relative FP centered around their respective pooled models in (6):

$$\begin{aligned}
\mathbf{T}_{si*} &\overset{ind}{\sim} \text{Multinomial}(n_{si}, \mathbf{\Phi}_{si*}) \text{ with } \phi_{sij} = (1 - \phi_{sii})q_{sij} \quad \forall i, \\
\phi_{sii} &\overset{ind}{\sim} \text{Beta}(0.5 + \gamma\phi_{ii}, 0.5 + \gamma(1 - \phi_{ii})) \quad \forall i \text{ with } f, \gamma > 0, \\
\mathbf{q}_{si*} &\overset{ind}{\sim} \text{Dir}(0.5 + \delta\mathbf{q}_{i*}) \quad \forall i \text{ with } g, \delta > 0.
\end{aligned} \tag{7}$$

We complete the hierarchy by setting the same priors for the pooled parameters ϕ_{ii} , \mathbf{q}_{i*} , a_i and $\boldsymbol{\alpha}$ as in (6). To account for heterogeneity across countries, ϕ_{sii} and \mathbf{q}_{si*} can be interpreted as the country-specific *random effects* of sensitivities and relative FP. The random effects are respectively distributed according to Beta and Dirichlet distributions and pivot around the respective *fixed effects* from the homogeneous model (6). The deviations of random effects from fixed effects quantify the *degree of heterogeneity*.

The heterogeneous model (7) subsumes the homogeneous model (6) as a specific instance as $\gamma, \delta \rightarrow \infty$. Conversely, as $\gamma, \delta \downarrow 0$, the random effects are distributed independently as the non-informative priors $\text{Beta}(0.5, 0.5)$ and $\text{Dir}(0.5, \dots, 0.5)$, respectively. In this case, no information is shared between countries and it is analogous to modeling misclassifications separately for each country. This framework thus encompasses separate country-specific modeling as a special case. For the intermediate scenario with some heterogeneity, the fixed effects capture the average misclassification rates common across the countries, and the heterogeneity is accounted for by the variability around them. Through γ and δ , the framework thus coherently includes varied degrees of heterogeneity

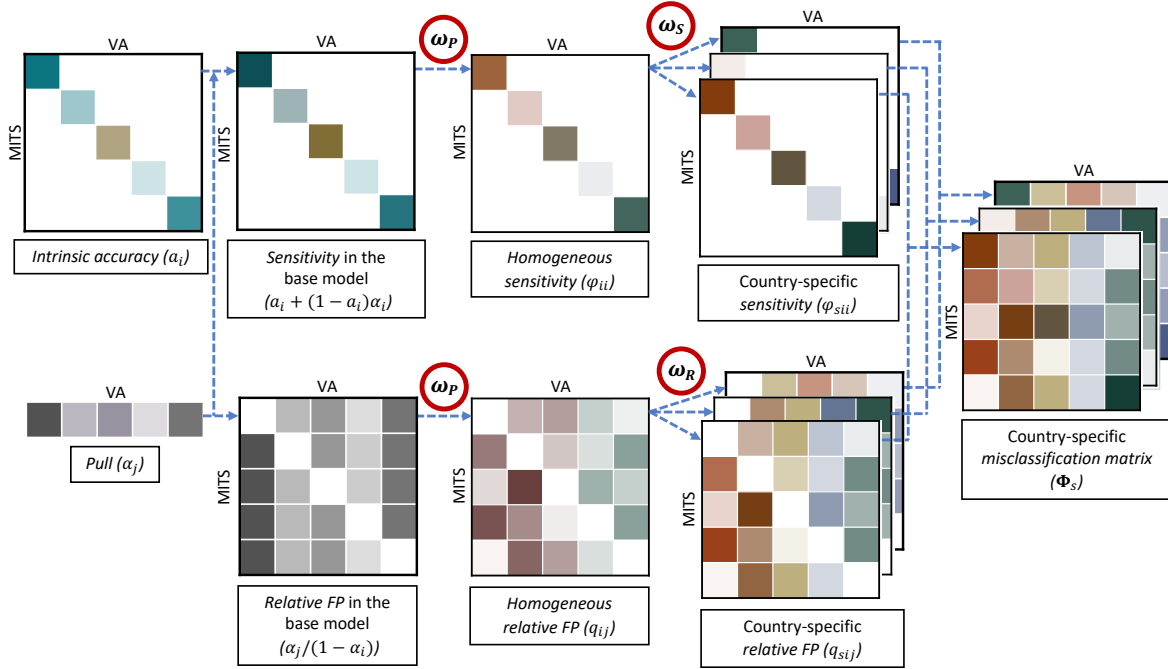


Figure 4: A schematic diagram of country-specific misclassification modeling framework.

in a nested structure.

Figure 4 presents a schematic of the proposed nested framework of the models with progressively increasing complexity. The heterogeneous model subsumes the homogeneous model which in turn incorporates the base model as a special case.

3.4 Interpretable Model Parameters

All parameters in the proposed framework are interpretable. The ϕ_{ij} 's and ϕ_{sij} 's are homogeneous and country-specific misclassification rates. The parameters specifying intrinsic accuracy (a_i) and systematic preference or pull (α_j) in the base model provide an understanding of the latent mechanism dictating the VA algorithm's misclassifications. The extensions to the homogeneous model (6) and the heterogeneous model (7) are respectively controlled by dispersion parameters (κ, λ) and (γ, δ) which have the following interpretation.

Dispersion parameters in Beta or Dirichlet priors carry the interpretation of prior sample sizes for *Binomial* or *Multinomial* data. Thus κ and λ can be interpreted as the *total prior sample size* for the prior that the pooled misclassification rates are generated from the base model. Similarly, γ and δ provide the prior sample size for a homogeneous prior for the heterogeneous misclassification rates. Following this we parameterize them as

$$\kappa = 2\omega_P, \quad \lambda = (C - 1)\omega_P, \quad \gamma = 2\omega_S \quad \text{and} \quad \delta = (C - 1)\omega_R, \quad (8)$$

where ω_P , ω_S , and ω_R are prior sample sizes for each category (2 categories for sensitivity representing correct or incorrect match, and $C - 1$ categories for relative FP representing false positive causes). Thus ω_P , ω_S , and ω_R are effect sizes of the framework and they respectively control the *pull strength* and the degrees of homogeneity in sensitivity and relative FP. A large ω_P indicates a *strong pull* – strong shrinkage towards the base model with systematic preference or pull, whereas a small value suggests *no pull* – an absence of structure in the misclassification rates. A large value of ω_S suggests homogeneity, favoring a strong shrinkage of the country-specific sensitivities ϕ_{sii} towards the pooled sensitivities ϕ_{ii} . A similar interpretation holds for ω_R for the country-specific relative FP q_{sij} .

3.5 Shrinkage Priors on Effect Sizes for Pull and Homogeneity

Considering the significance of dispersion parameters ω_P , ω_S , and ω_R in regulating the pull strength and degree of homogeneity, we propose to learn them from the data. In a Bayesian approach, this necessitates assigning priors for each of them. Specifically, we utilize shrinkage priors to favor a model with lower complexity, allowing more precise estimation even in low-sample size settings. We transform the effect sizes to $[0, 1]$ using the mapping $f(x) = 1/(1 + x)$ and assume that the transformed effect sizes are independently distributed as $\text{Beta}(\varepsilon, \varepsilon)$, for $\varepsilon \in (0, 1)$. On the transformed scale, 0 signifies the lowest complexity (strong pull and homogeneity) while the highest complexity corresponds to 1 (no pull and heterogeneity). With modes at 0 and 1, the

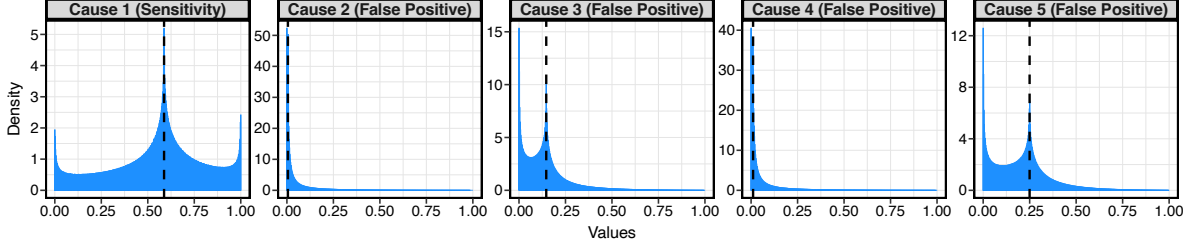


Figure 5: Conditional prior on misclassification rates in the homogeneous model (6) given the base model parameters and the Beta(0.5, 0.5) prior on pull strength (ω_P). Vertical dashed lines indicate the respective values in the base model (1).

prior allocates more probability near the two interpretable extremes. This encourages the model to shrink towards simplicity in low-sample size settings while being adaptable to a higher complexity if supported by data.

Figure S3 in the supplement shows an example of the prior for $\varepsilon = 0.5$. On the transformed scale, it assigns 50% probability outside (0.15, 0.85) and distributes the rest of the probability roughly evenly within the interval. On the original scale, this is equivalent to having at least 5.5 prior samples for each cause or category to indicate a strong pull or homogeneity, and fewer than 0.15 observations for suggesting no pull or heterogeneity.

This choice of shrinkage prior on dispersion parameters implies a conditional shrinkage on misclassification rates. Figure 5 shows an example of the conditional prior implied on homogeneous misclassification rates ϕ_{ij} in the homogeneous model (6) given the base model parameters \mathbf{a} and $\boldsymbol{\alpha}$ and the Beta(0.5, 0.5) prior on ω_P . For sensitivities, the conditional prior is trimodal, with peaks at the base model, 0 (shrinkage to perfect misclassification) and 1 (shrinkage to perfect classification). For false positives, the conditional prior is bimodal shrinking either to the base model or to 0. The prior thus encourages a *continuous shrinkage* (CARVALHO et al., 2010; Park and Casella, 2008): concentrating around the base model (dashed vertical lines), perfect misclassification, or perfect classification (for sensitivities only). The same conditional prior is also assumed in (7) for country-specific misclassification rates ϕ_{sij} given their homogeneous values ϕ_{ij} .

When dealing with limited samples, it conveniently encourages a continuous adjustment in pull strength and degree of heterogeneity to favor a simpler model for misclassification rates, while allowing for evidence accumulation in support of a more complex model as the sample size increases. This dynamically adjusts the modeling complexity, providing an optimal balance to the bias-variance trade-off in country-specific estimation by utilizing both local and global misclassification patterns in a data-driven manner.

3.6 Extrapolation to Unobserved MITS Causes and Countries

On account of borrowing information across countries, our Bayesian hierarchical framework naturally allows VA misclassification rate predictions for countries not represented in the CHAMPS data. It also enables predicting misclassification rates for a CHAMPS country with unobserved MITS causes. This is quite common since CHAMPS is based on convenient sampling and certain countries frequently lack observations for some MITS causes. For either task, we can obtain predictive distributions of the misclassification rates as follows.

For the homogeneous model (6), misclassification rates for a new country are the same as the posterior distribution of pooled misclassification rates ϕ_{ij} . For the heterogeneous model (7), the posterior predictive distribution of sensitivity and relative FP in a new country s are given by draws

$$\begin{aligned}\phi_{sii}^{(r)} &\sim \text{Beta}\left(0.5 + 2\omega_S^{(r)}\phi_{ii}^{(r)}, 0.5 + 2\omega_S^{(r)}(1 - \phi_{ii}^{(r)})\right), \text{ and} \\ \mathbf{q}_{si*}^{(r)} &\sim \text{Dir}\left(0.5 + (C - 1)\omega_R^{(r)}\mathbf{q}_{i*}^{(r)}\right),\end{aligned}\tag{9}$$

where r denotes the r^{th} MCMC sample. Note that, the predictive distributions for a country are centered at their homogeneous values, and the uncertainties around them for sensitivity and relative FP are guided by the posterior information on degrees of heterogeneity ω_S and ω_R . So the predictions from homogeneous and heterogeneous models will have similar point estimates, but the latter will have higher uncertainty that accounts for heterogeneity.

4 Simulation Study

We conducted extensive simulation studies to assess the performance in the presence and absence of heterogeneity across countries. We considered three scenarios of a true misclassification matrix: (i) *homogeneous*: The same misclassification matrix for all countries as in (6), (ii) *partly-heterogeneous*: heterogeneity only in sensitivities achieved by setting δ or $\omega_R = \infty$ in (7), and, (iii) *fully-heterogeneous*: heterogeneity in both sensitivity and relative FP as in (7). In each scenario, we fit these three methods that are special cases of the proposed framework. See sections S3 and S4 in the Supplement for additional details.

Figure 6 presents the model comparison metrics in different true scenarios using the *widely applicable information criterion (WAIC)* and *Leave-one-out cross-validation information criterion (LOO-IC)*. For all methods, Figure S5 in the supplement compares *in* and *out-of-sample* performances averaged over MITS-VA cause pairs for all countries. Summarizing all figures we find that all methods perform similarly when the misclassification matrix is truly homogeneous. However, where sensitivities exhibit heterogeneity, the heterogeneous methods perform similarly to each other, and they both surpass the performance of the homogeneous model. Finally, in cases where the

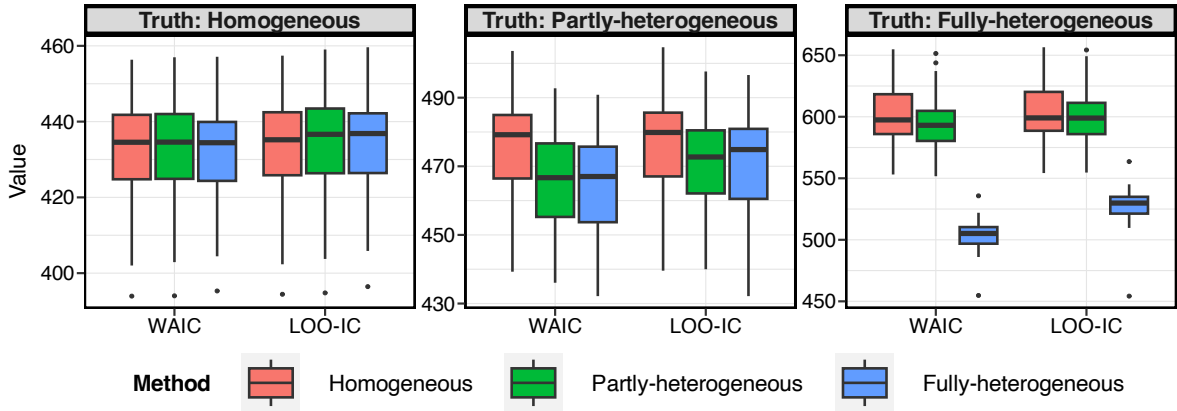


Figure 6: The box-plots of widely applicable information criterion (WAIC) and Leave-one-out cross-validation information criterion (LOO-IC) from 50 replications. Panels indicate true simulation scenarios. Lower values are better.

misclassification matrix is fully-heterogeneous, the fully-heterogeneous method significantly outperforms both the homogeneous and partly-heterogeneous methods. This highlights the fully-heterogeneous method’s flexibility in adapting to different situations and demonstrates its efficacy in capturing heterogeneity.

5 Country-resolved Misclassification Rates of InSili-coVA

Here we revisit the CHAMPS data introduced in Section 2 and implement the proposed country-specific model to estimate InSili-coVA’s misclassification rates for neonatal deaths.

5.1 Misclassification Rate Estimates

We implemented the three methods as outlined in Section 4 but focus our comparison on homogeneous and fully-heterogeneous methods for brevity, unless stated otherwise. In Figure 7 we present the point (posterior mean) and uncertainty estimates (95% credible interval) of country-specific misclassification rates from the two methods and compare them with the observed data. When strong evidence of heterogeneity is absent in observed rates, the estimates from fully-heterogeneous method closely resemble the homogeneous estimates. Examples include sensitivity and false positives for MITS cause prematurity. On the other hand, if there is a substantial heterogeneity in observed rates, the fully-heterogeneous estimates better match the observed rates as compared to homogeneous estimates. This is seen for sensitivities of IPRE and false positive rates of IPRE-prematurity in Mozambique and Sierra Leone. Collectively, the fully-heterogeneous model yields more accurate in-sample estimates in the presence of heterogeneity, while

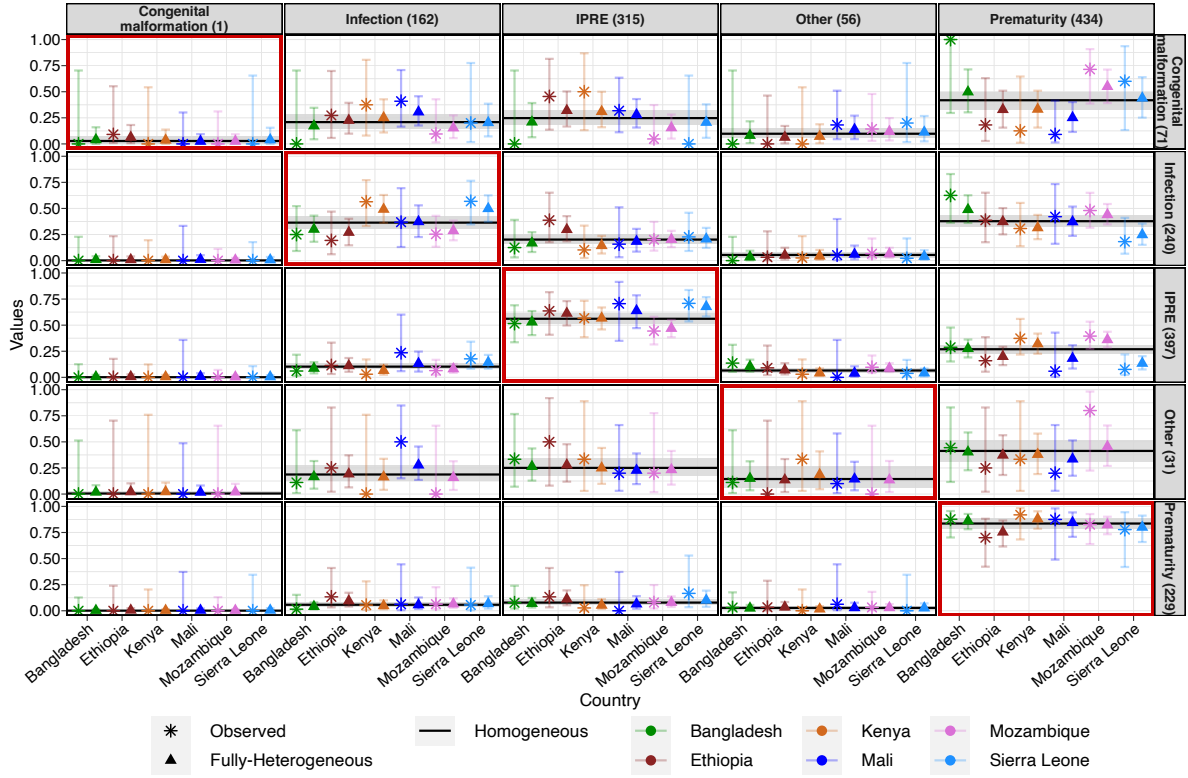


Figure 7: Comparison of observed misclassification rates with in-sample point (posterior mean) and uncertainty (95% credible interval) estimates from homogeneous and fully-heterogeneous models. Rows and columns refer to MITS and VA-predicted causes.

demonstrating comparable performance to the homogeneous model in situations where heterogeneity is relatively insignificant.

5.2 Model Comparison

Figure 8 presents the model comparison metrics between the fully-heterogeneous model and the homogeneous model for both point and interval estimation. Point estimates are compared using absolute bias in posterior means and 95% credible intervals are evaluated using interval scores (Gneiting and Raftery, 2007). The results overwhelmingly favor the heterogeneous model. Combined across countries, it reduced bias for 73% cause pairs. For half of the cause pairs the bias decreased by at least 44%, with reductions as high as 98% (MITS cause congenital malformation, VA cause prematurity in Mali). Only for the first columns of the misclassification matrices (corresponding to some MITS cause, and VA cause congenital malformation), the homogeneous model has slightly less bias. This is because InSilicoVA does not predict congenital malformation, so the observed misclassification rates in this column are exactly 0. The homogeneous model on account of pooling data is less reliant on the prior and estimates are also nearly zero. For the heterogenous model, the estimates are also very close to zero but there is still bias on

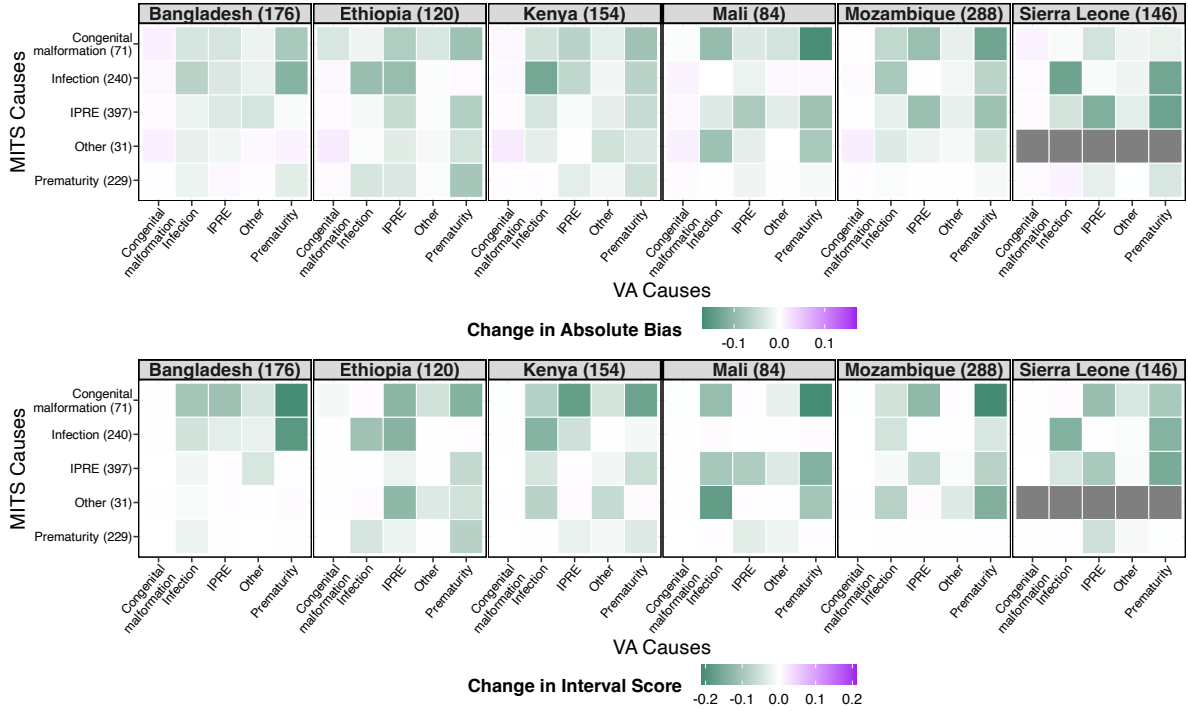


Figure 8: The figure compares the change in absolute bias in posterior means (*top panel*) and interval scores of 95% credible intervals (*bottom panel*) in the fully-heterogeneous method compared to the homogeneous method. Rows and columns are MITs and VA causes. Negative values are better (green color) indicating reduction in bias / interval score.

account of being more influenced by the prior which gives some mass away from zero.

The heterogeneous model also reduced interval scores for 57% cause pairs across countries. There was at least 87% reduction in scores for 50% cause pairs, with reductions as high as 98%. Additionally, Figure S7 in the supplement displays the LOO-IC and WAIC for all three methods. Compared to the homogeneous method, the partly-heterogeneous method enhances the information criteria by 6–7%. However, the fully-heterogeneous method outperforms all, improving the criteria by 5–8% over partly-heterogeneous and an impressive 11–15% over the homogeneous method. In summary, the fully-heterogeneous model produces more accurate in-sample estimates than the homogeneous model.

5.3 Estimates of Effect Size, Intrinsic Accuracy, and Pull

Estimates of Effect Sizes ω_P , ω_S , ω_R . We discuss estimates of key modeling parameters that define the proposed framework. Figure 9 compares posterior densities of effect size estimates from three different models. With effect sizes carrying the interpretation of prior sample sizes per cause or category, the estimates must be compared

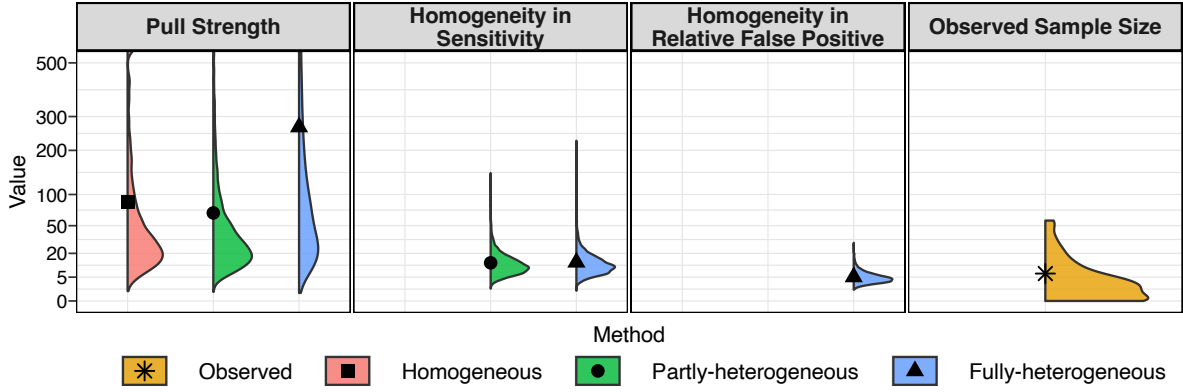


Figure 9: Three panels on the left show posteriors of effect sizes from three models. Larger values indicate a stronger effect. The last panel displays the frequency distribution of sample sizes observed across cause pairs and countries for the comparative analysis of effect size magnitude. Black points denote means of respective distributions. *For clear representation, the y-axis is plotted on the square root scale and is restricted to the range of means.*

in conjunction with sample sizes observed across cause pairs and countries (Figure 9, last panel).

First, we note that the effect size estimates for parameters common to the models are generally consistent with each other. For example, the posterior density pull strength ω_P , which dictates the shrinkage towards the base model in all 3 models, have roughly similar shapes and modes. This is also seen for ω_S controlling homogeneity in the sensitivity. This underscores the validity of the adaptive nested structure of the framework. Second, the estimates of ω_P are significantly higher (posterior means range 75–400) than the maximum observed sample size (57). This indicates very strong evidence towards the base model structure indicating systematic preference underlying InSilicoVA’s misclassification mechanism. Third, the estimate of ω_S is significantly lower (posterior means ≈ 12) compared to that of pull strength and the maximum sample size. This indicates a strong presence of heterogeneity in sensitivities. Finally, the estimates for the degree of homogeneity in relative FP (ω_R) is even lower (posterior mean ≈ 5) than ω_S . This implies significant heterogeneity in InSilicoVA’s relative FP across countries, with a more pronounced degree compared to that in sensitivity. Together, this suggests a strong systematic preference and a pronounced presence of heterogeneity across different countries in InSilicoVA’s misclassification rates.

Estimates of Intrinsic Accuracy (a) and Pull (α). Figure 10 showcases the posteriors of intrinsic accuracies a_i ’s and pulls α_j ’s from the fully-heterogeneous method, and they offer two key findings. Note that, in the absence of systematic preference, an algorithm would uniformly misclassify all causes, implying an *average pull* of $1/5$ (green dashed line) for each cause. Contrary to this, the pull estimates in Figure 10a suggest that the algorithm overstates prematurity and suppresses congenital malformation and

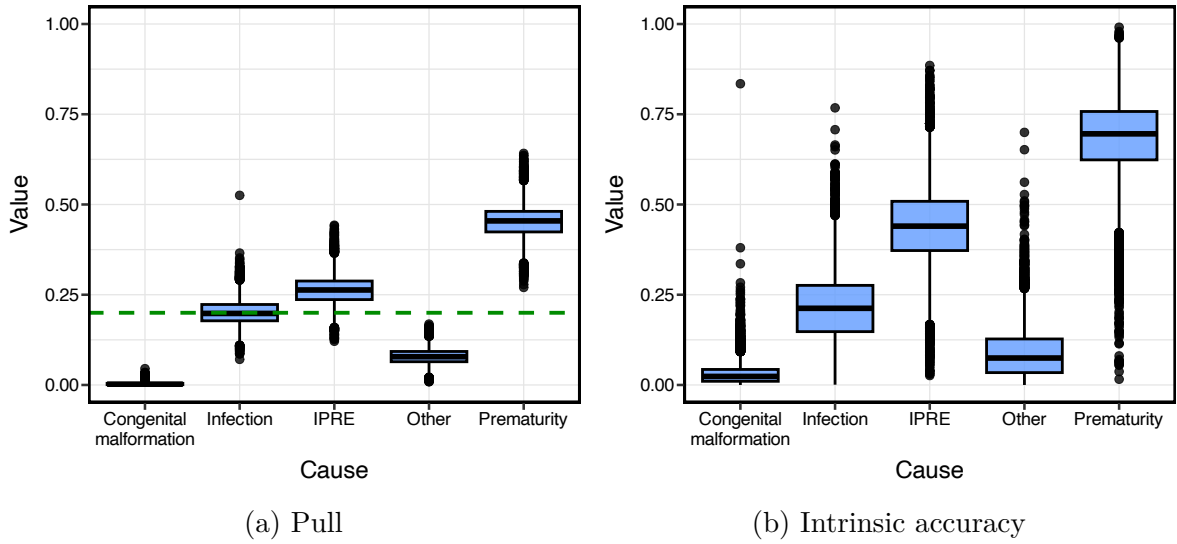


Figure 10: The posterior of intrinsic accuracies and pull for InSilicoVA among neonatal deaths in CHAMPS. The horizontal dashed line in (b) corresponds to no preference with a uniform pull of 1/5 for each cause.

other, clearly demonstrating a presence of systematic preference. We display intrinsic accuracy estimates for all causes in Figure 10b. While observed sensitivities are induced by both intrinsic accuracy and pull, the figure shows that intrinsic accuracy dominates the influence for most causes, with prematurity having the highest intrinsic accuracy, followed by IPRE.

5.4 Extrapolation Performance

For out-of-sample comparison, we train methods by omitting one country at a time and assess predictive accuracy with respect to observed rates in the excluded country. Figure S6 in the supplement compares out-of-sample point (predictive mean) and uncertainty predictions (95% prediction interval) from homogeneous and fully-heterogeneous methods. The point predictions from the two methods are similar and it conforms to the discussion in Section 3.6. The homogeneous model provides narrower intervals compared to the fully-heterogeneous model as it ignores heterogeneity. The intervals from the fully-heterogeneous method account for heterogeneity and are more accurate. This performance difference is evident in the sensitivity of infection and false positive rates of IPRE-prematurity.

Figure 11 formally compares the uncertainty quantification. Compared to the homogeneous method, the fully-heterogeneous model reduces the interval scores for 55% cause pairs across countries. There is at least 77% reduction for half of the cause pairs, with reductions as high as 94%. This collectively demonstrates the advantages of the fully-heterogeneous method in offering more accurate out-of-sample predictions.

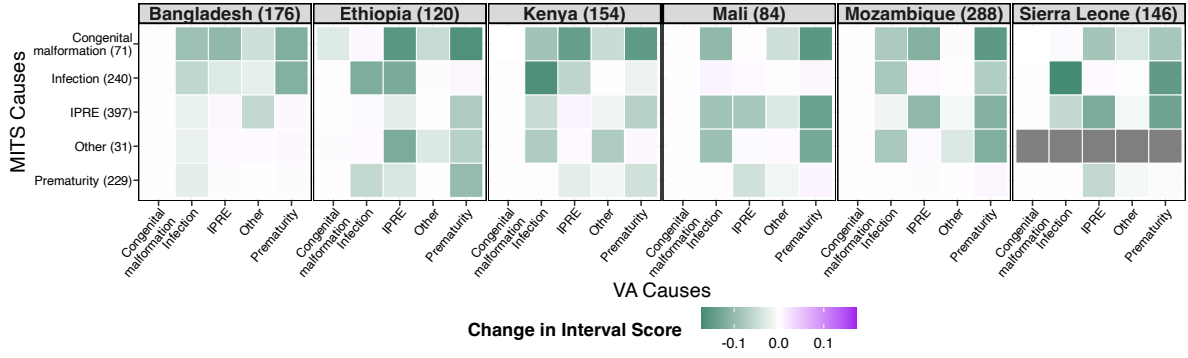


Figure 11: The figure compares differences in interval scores of 95% prediction intervals in the fully-heterogeneous model compared to the homogeneous. Rows and columns are MITS and VA causes. Smaller values are better (green color), indicating more reduction in scores.

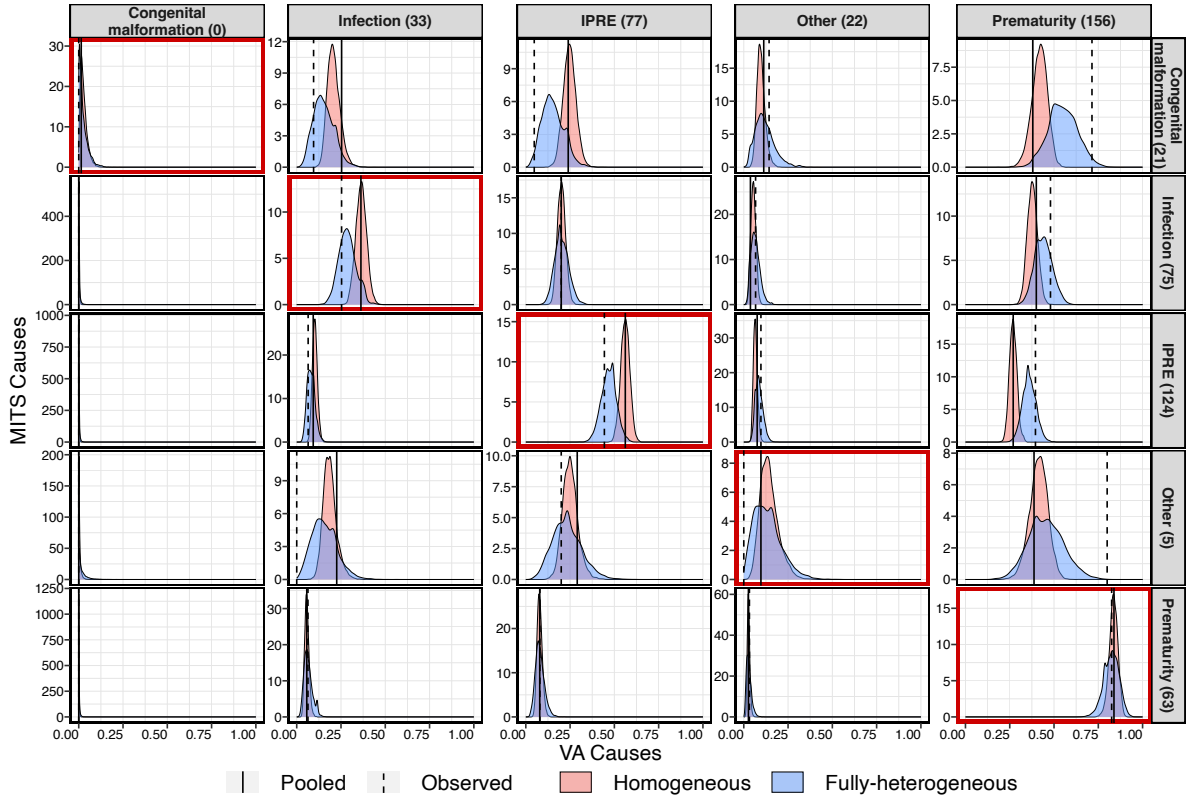


Figure 12: Comparison of misclassification rate estimates in Mozambique from homogeneous and fully-heterogeneous models. The solid vertical lines denote the proportions pooled across countries while the dashed lines denote that observed in Mozambique. The numbers enclosed in panel headings are sample sizes in Mozambique.

5.5 Misclassification Matrix Estimate in Mozambique

Assuming homogeneous misclassification rates, [Fiksel et al. \(2023\)](#) and [Gilbert et al. \(2023\)](#) estimated Mozambique’s misclassification matrix by pooling CHAMPS data from all countries. Figure 12 contrasts the uncertainty quantified posterior estimates of misclassification rates in Mozambique derived from our homogeneous (red) and fully-heterogeneous (blue) models. When for an MITS-VA cause pair the empirical misclassification rate in Mozambique (dashed line) significantly differs from the pooled empirical rate (solid line), and an adequate number of samples is available, the fully-heterogeneous method provides a more precise estimate. This is evident in sensitivities for infection and IPRE, and false positives for congenital malformation-infection and IPRE-prematurity. When sample sizes are insufficient, this approach enhances the stability of country-specific estimates by shrinking them towards the pooled estimate. This underscores the adaptive nature of the proposed framework in providing more representative country-specific estimates in the presence of enough evidence while shrinking towards the pooled estimate otherwise to improve precision.

6 Discussion

Accurate misclassification rate estimation for VA algorithms is pivotal in obtaining valid CSMF estimates based on VA-calibration. The labeled MITS-VA COD data collected in CHAMPS is a vital resource in this context. Although prior research assumes the same misclassification rates for all countries, our findings expose substantial local heterogeneity and emphasize the need for addressing it. With the number of parameters growing as a quadratic in the number of causes and linearly in the number of countries, the limited availability of MITS cases poses a challenge in obtaining meaningful country-specific estimates.

We introduced a novel framework for heterogeneous modeling of misclassification matrices with three key components: (i) the base model to account for the systematic preference of VA algorithms, (ii) the exact error matrix decomposition into sensitivities and relative FP to generalize the base model, and (iii) the hierarchically-defined nested Bayesian framework to incorporate heterogeneity. The base model introduces the concept of pull to quantify systematic preferences for certain causes. Theorem 3.1 characterizes its manifestation in terms of constant misclassification odds. The nested structure enables the framework to systematically expand from a simple homogeneous model to a complex country-specific model in a data-driven manner. In the absence of evidence, the shrinkage prior on effect sizes encourages lower complexity effectively compensating for limited MITS cases.

Findings from this research have immediate and future implications for global health. In the short term, the Mozambique-specific misclassification matrix estimated here will be combined with VA-only data collected in COMSA-Mz to produce calibrated CSMF estimates. For different VA algorithms and age groups, we will perform comparative analyses of misclassification rates and resulting CSMF estimates. In the longer term,

these estimates will be used to calibrate VA data from 100 studies for the next set of regional and national under-5 CSMF estimates for the Sustainable Development Goals (Perin et al., 2022).

In numerous scientific challenges, the mechanisms behind data generation are either unknown or cannot be guaranteed. The notion of misclassification thus pervades various domains in Statistics, extending much beyond cause-of-death analyses. Statistical inference for association studies using *electronic health records (EHR)* is an example in health-related research where outcomes are often misclassified (Beesley and Mukherjee, 2022; Sinnott et al., 2014). More recently, we are seeing rapid advancements in *large language models* and other computer-coded algorithms across *machine learning* and *artificial intelligence* that do not perfectly capture truth. In this regard, *transfer learning* has become increasingly relevant which aims at improving a *target learner*’s performance on *target domains* by transferring the knowledge contained in different but related *source domains* (Wang et al., 2018; Zhuang et al., 2021). Given the inherent nature of misclassification, it timely presents opportunities for us to extend the fundamental concepts presented in this research to diverse scientific problems. Instances such as these, among many others, underscore that the crux of the addressed issue resides at the intersection of multiple active and promising scientific problems. Exploring and expanding these concepts, as well as delving into other facets to address them, presents an intriguing avenue for future research.

Supplementary Materials

Proofs of theoretical results, simulation details, and additional figures that generate country-specific misclassification matrix estimates are provided in the Supplementary Materials. Codes will be added to the existing *VA-calibration* R package on CRAN.

Acknowledgement

S.P., S.Z., A.D. were supported by the Bill and Melinda Gates Foundation Grant INV-034842. D.B. received support from the Bill and Melinda Gates Foundation Grant OPP1126780. The authors are grateful to Emily Wilson and Dr. Henry Kalter for processing the CHAMPS data. The findings and conclusions in this report are those of the authors and do not necessarily represent the views of the US Centers for Disease Control and Prevention.

References

Adair, T. and Lopez, A. D. (2018). Estimating the completeness of death registration: An empirical method. *PLOS ONE*, 13(5):1–19.

- Bassat, Q., Castillo, P., Martínez, M. J., Jordao, D., Lovane, L., Hurtado, J. C., Nhampossa, T., Santos Ritchie, P., Bandeira, S., Sambo, C., et al. (2017). Validity of a minimally invasive autopsy tool for cause of death determination in pediatric deaths in mozambique: an observational study. *PLoS medicine*, 14(6):e1002317.
- Beesley, L. J. and Mukherjee, B. (2022). Statistical inference for association studies using electronic health records: handling both selection bias and outcome misclassification. *Biometrics*, 78(1):214–226.
- Blau, D. M., Caneer, J. P., Philipsborn, R. P., Madhi, S. A., Bassat, Q., Varo, R., Mandomando, I., Igunza, K. A., Kotloff, K. L., Tapia, M. D., et al. (2019). Overview and development of the child health and mortality prevention surveillance determination of cause of death (decode) process and decode diagnosis standards. *Clinical Infectious Diseases*, 69(Supplement_4):S333–S341.
- Carshon-Marsh, R., Aimone, A., Ansumana, R., Swaray, I. B., Assalif, A., Musa, A., Meh, C., Smart, F., Fu, S. H., Newcombe, L., et al. (2022). Child, maternal, and adult mortality in sierra leone: nationally representative mortality survey 2018–20. *The Lancet Global Health*, 10(1):e114–e123.
- CARVALHO, C. M., POLSON, N. G., and SCOTT, J. G. (2010). The horseshoe estimator for sparse signals. *Biometrika*, 97(2):465–480.
- Clark, S. J., Li, Z., and McCormick, T. H. (2018). Quantifying the contributions of training data and algorithm logic to the performance of automated cause-assignment algorithms for verbal autopsy. *arXiv preprint arXiv:1803.07141*.
- Datta, A., Fiksel, J., Amouzou, A., and Zeger, S. L. (2020). Regularized Bayesian transfer learning for population-level etiological distributions. *Biostatistics*, 22(4):836–857.
- de Savigny, D., Riley, I., Chandramohan, D., Odhiambo, F., Nichols, E., Notzon, S., AbouZahr, C., Mitra, R., Cobos Muñoz, D., Firth, S., et al. (2017). Integrating community-based verbal autopsy into civil registration and vital statistics (crvs): system-level considerations. *Global health action*, 10(1):1272882.
- Fiksel, J., Datta, A., Amouzou, A., and Zeger, S. (2022). Generalized bayes quantification learning under dataset shift. *Journal of the American Statistical Association*, 117(540):2163–2181.
- Fiksel, J., Gilbert, B., Wilson, E., Kalter, H., Kante, A., Akum, A., Blau, D., Bassat, Q., Macicame, I., Gudo, E. S., Black, R., Zeger, S., Amouzou, A., and Datta, A. (2023). Correcting for verbal autopsy misclassification bias in cause-specific mortality estimates. *The American Journal of Tropical Medicine and Hygiene*, 108(5 Suppl):66–77.
- Garenne, M. (2014). Prospects for automated diagnosis of verbal autopsies. *BMC medicine*, 12:1–5.

- Gilbert, B., Fiksel, J., Wilson, E., Kalter, H., Kante, A., Akum, A., Blau, D., Bassat, Q., Macicame, I., Gudo, E. S., Black, R., Zeger, S., Amouzou, A., and Datta, A. (2023). Multi-cause calibration of verbal autopsy-based cause-specific mortality estimates of children and neonates in mozambique. *The American Journal of Tropical Medicine and Hygiene*, 108(5 Suppl):78–89.
- Gneiting, T. and Raftery, A. E. (2007). Strictly proper scoring rules, prediction, and estimation. *Journal of the American Statistical Association*, 102(477):359–378.
- Macicame, I., Kante, A., and Wilson, E. e. a. (2023). Countrywide mortality surveillance for action in mozambique: Results from a national sample-based vital statistics system for mortality and cause of death. *The American Journal of Tropical Medicine and Hygiene*, 108(5 Suppl):5–16.
- Menendez, C., Castillo, P., Martínez, M. J., Jordao, D., Lovane, L., Ismail, M. R., Carrilho, C., Lorenzoni, C., Fernandes, F., Nhampossa, T., et al. (2017). Validity of a minimally invasive autopsy for cause of death determination in stillborn babies and neonates in mozambique: an observational study. *PLoS medicine*, 14(6):e1002318.
- Mikkelsen, L., Phillips, D. E., AbouZahr, C., Setel, P. W., De Savigny, D., Lozano, R., and Lopez, A. D. (2015). A global assessment of civil registration and vital statistics systems: monitoring data quality and progress. *The Lancet*, 386(10001):1395–1406.
- Nichols, E. K., Byass, P., Chandramohan, D., Clark, S. J., Flaxman, A. D., Jakob, R., Leita, J., Maire, N., Rao, C., Riley, I., Setel, P. W., and on behalf of the WHO Verbal Autopsy Working Group (2018). The who 2016 verbal autopsy instrument: An international standard suitable for automated analysis by interval, insilicova, and tariff 2.0. *PLOS Medicine*, 15(1):1–9.
- Park, T. and Casella, G. (2008). The bayesian lasso. *Journal of the American Statistical Association*, 103(482):681–686.
- Perin, J., Mulick, A., Yeung, D., Villavicencio, F., Lopez, G., Strong, K. L., Prieto-Merino, D., Cousens, S., Black, R. E., and Liu, L. (2022). Global, regional, and national causes of under-5 mortality in 2000–19: an updated systematic analysis with implications for the sustainable development goals. *The Lancet Child & Adolescent Health*, 6(2):106–115.
- Salzberg, N. T., Sivalogan, K., Bassat, Q., Taylor, A. W., Adedini, S., El Arifeen, S., Assefa, N., Blau, D. M., Chawana, R., Cain, C. J., Cain, K. P., Caneer, J. P., Garel, M., Gurley, E. S., Kaiser, R., Kotloff, K. L., Mandomando, I., Morris, T., Nyamthimba Onyango, P., Sazzad, H. M. S., Scott, J. A. G., Seale, A. C., Siteo, A., Sow, S. O., Tapia, M. D., Whitney, E. A., Worrell, M. C., Zielinski-Gutierrez, E., Madhi, S. A., Raghunathan, P. L., Koplan, J. P., Breiman, R. F., Health, C., and Consortium, M. P. S. C. M. (2019). Mortality surveillance methods to identify and

- characterize deaths in child health and mortality prevention surveillance network sites. *Clinical Infectious Diseases*, 69(Supplement_4):S262–S273.
- Setel, P. W., Sankoh, O., Rao, C., Velkoff, V. A., Mathers, C., Gonghuan, Y., Hemed, Y., Jha, P., and Lopez, A. D. (2005). Sample registration of vital events with verbal autopsy: a renewed commitment to measuring and monitoring vital statistics. *Bulletin of the World Health Organization*, 83:611–617.
- Sinnott, J. A., Dai, W., Liao, K. P., Shaw, S. Y., Ananthakrishnan, A. N., Gainer, V. S., Karlson, E. W., Churchill, S., Szolovits, P., Murphy, S., et al. (2014). Improving the power of genetic association tests with imperfect phenotype derived from electronic medical records. *Human genetics*, 133:1369–1382.
- Soleman, N., Chandramohan, D., and Shibuya, K. (2006). Verbal autopsy: current practices and challenges. *Bulletin of the World Health Organization*, 84(3):239–245.
- Wang, B., Yao, Y., Viswanath, B., Zheng, H., and Zhao, B. Y. (2018). With great training comes great vulnerability: Practical attacks against transfer learning. In *27th USENIX Security Symposium (USENIX Security 18)*, pages 1281–1297, Baltimore, MD. USENIX Association.
- Wang, H., Abajobir, A. A., Abate, K. H., Abbafati, C., Abbas, K. M., Abd-Allah, F., Abera, S. F., Abraha, H. N., Abu-Raddad, L. J., Abu-Rmeileh, N. M., et al. (2017). Global, regional, and national under-5 mortality, adult mortality, age-specific mortality, and life expectancy, 1970–2016: a systematic analysis for the global burden of disease study 2016. *The Lancet*, 390(10100):1084–1150.
- Zhuang, F., Qi, Z., Duan, K., Xi, D., Zhu, Y., Zhu, H., Xiong, H., and He, Q. (2021). A comprehensive survey on transfer learning. *Proceedings of the IEEE*, 109(1):43–76.

Supplement: Modeling Structure and Country-specific Heterogeneity in Misclassification Matrices of Verbal Autopsy-based Cause of Death Classifiers

Sandipan Pramanik¹, Scott Zeger¹, Dianna Blau², and Abhirup Datta¹

¹Department of Biostatistics, Johns Hopkins University

²Global Health Center, US Centers for Disease Control and Prevention

December 7, 2023

Abstract

In this supplementary file, we provide some technical details and additional materials for the main article.

S1 Proof of Theorem 3.1 in The Main Article

Proof of ‘if’ part. Let us fix an MITS cause i arbitrarily. The constant odds condition from Theorem 3.1 in the main article implies that, for some positive η_{jk} for $j \neq k$,

$$\frac{\phi_{ij}}{\phi_{ik}} = \eta_{jk}, \quad \forall i \text{ and } j \neq k \neq i.$$

Being odds, η_{jk} ’s also satisfy

$$\eta_{jk}\eta_{kl} = \eta_{jl}, \quad \forall j \neq k \neq l.$$

Setting $l = C$ without loss of generality we get

$$\eta_{jk} = \frac{\eta_{jC}}{\eta_{kC}} = \frac{\theta_j}{\theta_k}, \quad \forall j \neq k,$$

where θ_j ’s are positive. Combining this with the decomposition (4) in the main article we get

$$\frac{\phi_{ij}}{\phi_{ik}} = \frac{q_{ij}}{q_{ik}} = \frac{\theta_j}{\theta_k} \Rightarrow q_{ij} = \frac{\theta_j}{\theta_k} q_{ik}, \quad \forall i \text{ and } j \neq k \neq i.$$

Using $\sum_{j \neq i} q_{ij} = 1$, we obtain

$$q_{ij} = \frac{\theta_j}{\sum_{l \neq i} \theta_l}, \quad \forall i \text{ and } j \neq i.$$

Defining the pull as $\alpha_j = \theta_j / \sum_l \theta_l$ completes the proof.

Proof of ‘only if’ part. Recall from (5) in the main article that, the relative FP q_{ij} in the base model equals to $\alpha_j/(1 - \alpha_i)$. Together with the decomposition (4), this yields

$$\frac{\phi_{ij}}{\phi_{ik}} = \frac{\alpha_j}{\alpha_k}, \quad \forall j, k \neq i.$$

Defining $\alpha_j = \theta_j$ completes the proof.

S2 Proof of Proposition 3.1 in The Main Article

According to (1) in the main article, the classification probabilities in the base model are

$$\begin{aligned} \phi_{ii} &= a_i + (1 - a_i)\alpha_i \quad \forall i, \\ \phi_{ij} &= (1 - a_i)\alpha_j \quad \forall j \neq i, \end{aligned}$$

where $\mathbf{a} = (a_1, \dots, a_C)^T$ are intrinsic accuracies with $a_i \in (0, 1)$, and $\boldsymbol{\alpha} = (\alpha_1, \dots, \alpha_C)^T$ denotes the pull which lies in the C -dimensional simplex.

We prove the proposition by contradiction. Suppose, the base model likelihood is not identifiable with respect to \mathbf{a} and $\boldsymbol{\alpha}$. So there exists intrinsic accuracies $\mathbf{a}_1 \neq \mathbf{a}_2$, and pulls $\boldsymbol{\alpha}_1 \neq \boldsymbol{\alpha}_2$ that yields the same likelihood. Mathematically,

$$\begin{aligned} a_{1i} + (1 - a_{1i})\alpha_{1i} &= a_{2i} + (1 - a_{2i})\alpha_{2i} \quad \forall i, \\ (1 - a_{1i})\alpha_{1j} &= (1 - a_{2i})\alpha_{2j} \quad \forall j \neq i. \end{aligned} \tag{S1}$$

Without loss of generality, fix $i = 1$. For $j = 2, \dots, C$, (S1) implies

$$\alpha_{1j} = \frac{(1 - a_{21})}{(1 - a_{11})}\alpha_{2j} = k_1\alpha_{2j}, \quad \text{where} \quad k_1 = \frac{1 - a_{21}}{1 - a_{11}}. \tag{S2}$$

Since $\sum_{j=1}^C \alpha_{1j} = 1$, this implies $\alpha_{11} = 1 - \sum_{j=2}^C \alpha_{1j} = 1 - k_1(1 - \alpha_{21})$. Fixing $i = 2$, we similarly get

$$\alpha_{1j} = k_2\alpha_{2j}, \quad \forall j = 1, 3, \dots, C, \quad \text{with} \quad k_2 = \frac{1 - a_{22}}{1 - a_{12}}, \tag{S3}$$

$$\alpha_{12} = 1 - \sum_{j \neq 2} \alpha_{1j} = 1 - k_2(1 - \alpha_{22}). \tag{S4}$$

Equating (S2) and (S3) for $j = 3$ implies $k_1 = k_2 = k$, say. Finally, equating α_{12} from (S2) with (S4) we get

$$k\alpha_{22} = 1 - k(1 - \alpha_{22}) \Rightarrow k = 1.$$

This implies $\mathbf{a}_1 = \mathbf{a}_2$ and $\boldsymbol{\alpha}_1 = \boldsymbol{\alpha}_2$.

S3 Default Prior Parameter Choices

We suggest using the following parameter values for default implementation of the framework (6)–(7) in the main article: $b = d = 1$ indicating the Uniform prior on intrinsic accuracies, $\mathbf{e} = \mathbf{1}$ assuming the Uniform prior on pull, and Beta(0.5, 0.5) on effect sizes (Please see Section 3.5 in

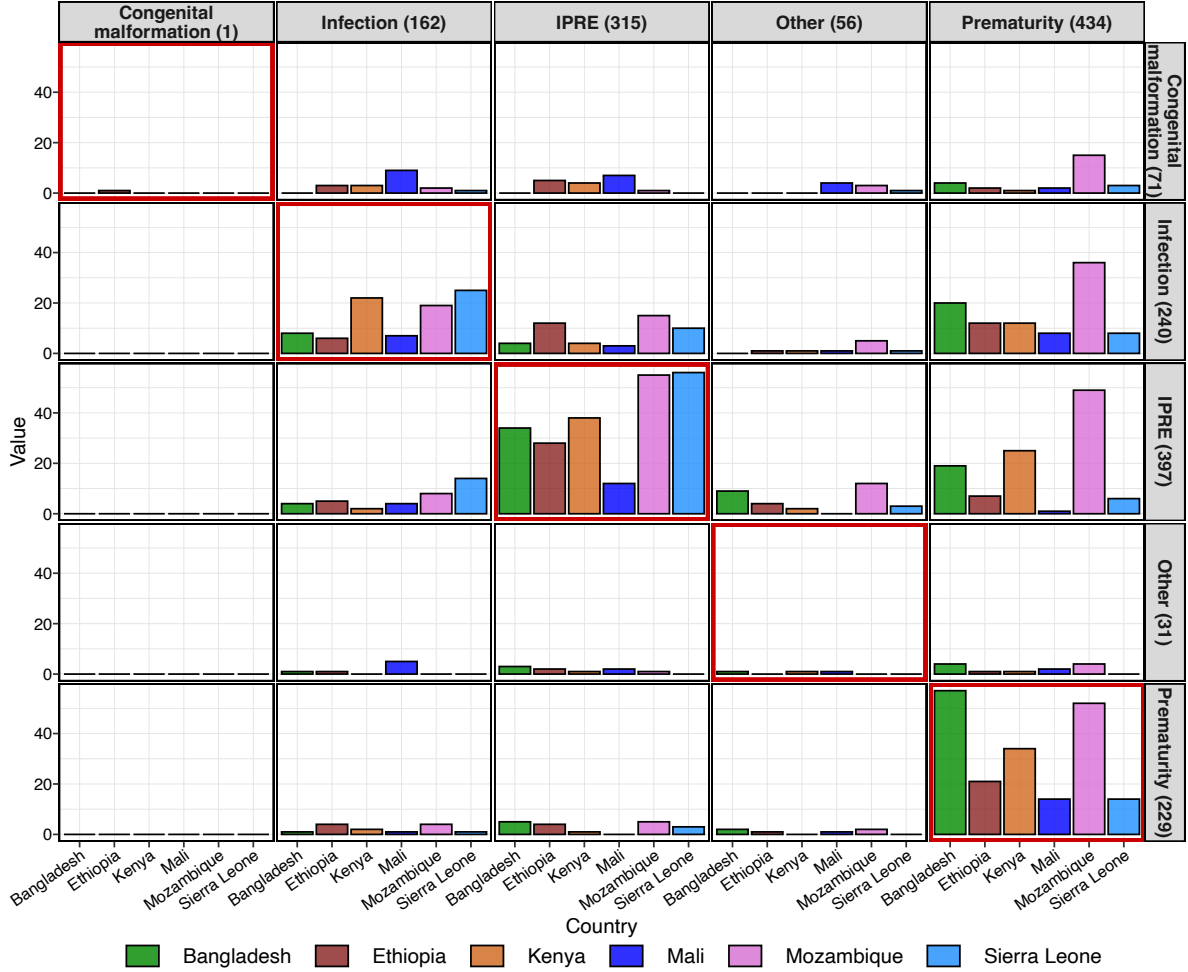


Figure S1: Neonatal deaths observed in the CHAMPS dataset for InSilicoVA across different MITS-VA cause pairs and countries. Rows and columns are MITS and VA-predicted causes. Numbers in parentheses denote the sample size.

the main article). Practitioners are advised to analyze the impact of prior parameter selections on their specific applications and customize them accordingly. Despite the desired continuous shrinkage, the implied marginal priors on classification rates for default choices are weakly informative, closely resembling the Jeffreys prior commonly recommended in the literature as a noninformative prior choice on Binomial and Multinomial probabilities (Please see Figure S4).

S4 Simulation Study

For simulating data, we mimic features of the data observed in CHAMPS and set the number of causes C to 5, the number of countries S to 6, and 50 MITS cases from each country. Finally, intrinsic accuracies (\mathbf{a}), pull (α), and effect sizes ω_P , ω_S and ω_R are set to their estimated values from the fully-heterogeneous model. Figure 9 in the main article shows that

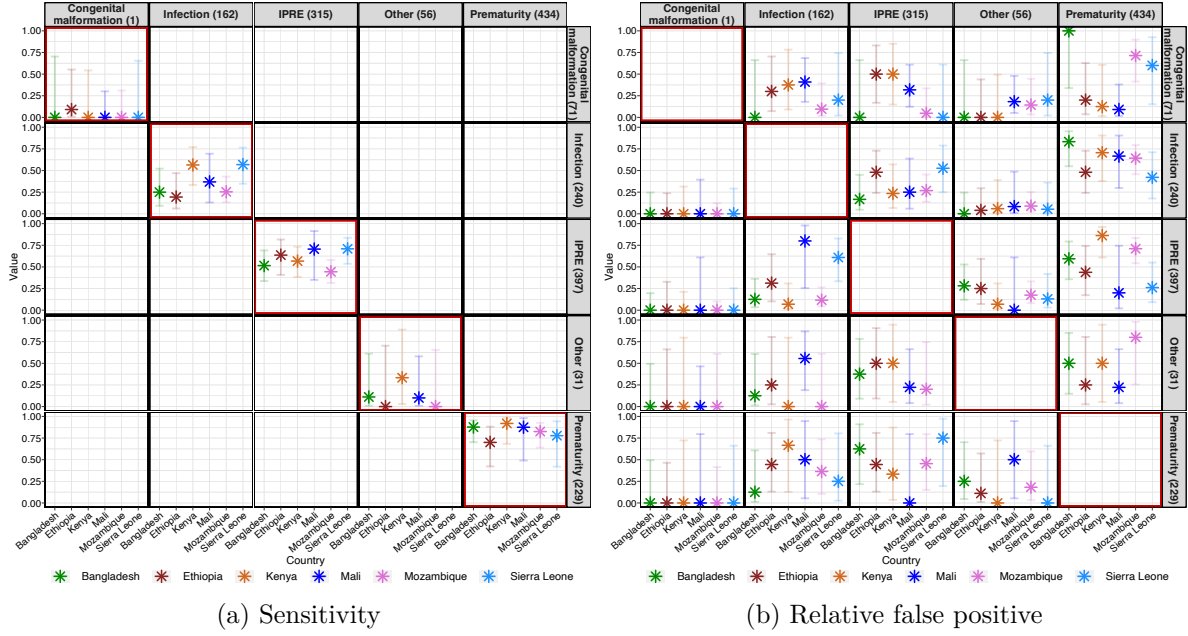


Figure S2: The exact decomposition of InsilicoVA’s observed classification proportions into sensitivities and relative false positives according to decomposition (4) in the main article.

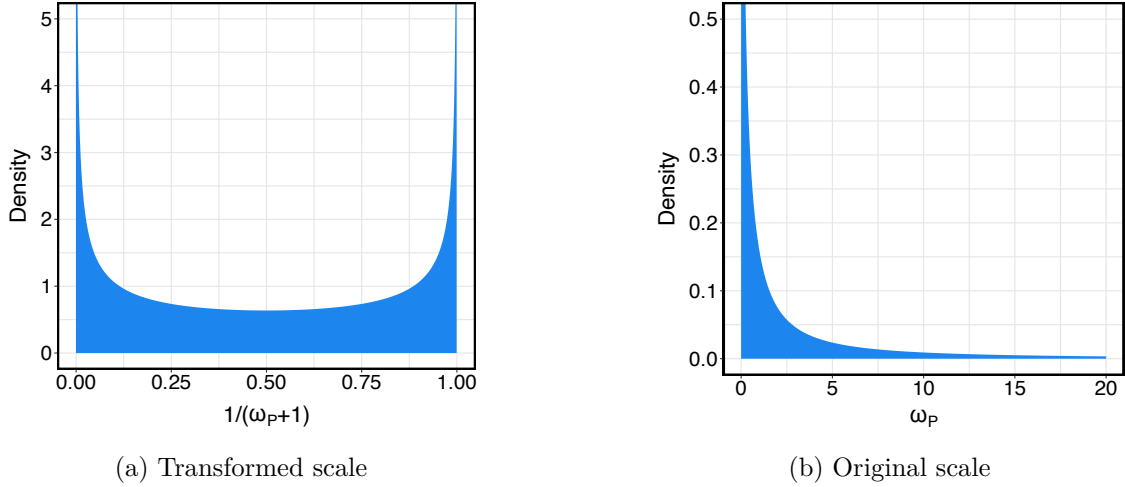


Figure S3: (a) on the left depicts the prior on transformed effect sizes for $\varepsilon = 0.5$. For the same choice, Figure (b) on the right presents the implied prior on the original scale.

the estimate for ω_S is significantly higher than that of ω_R . Consequently, this exhibits more heterogeneity in relative FP compared to sensitivities in the simulated data. Our modeling was conducted using the **Stan** software, and we employed the default prior parameter settings, as detailed in Section S3. We generated a total of 10,000 *Markov Chain Monte Carlo (MCMC)* samples, discarding the initial 5,000 samples as *burn-in*. The results from simulations were summarized across 50 replications.

For three methods outlined in Section 4 in the main article, Figure S5 compares their *in*

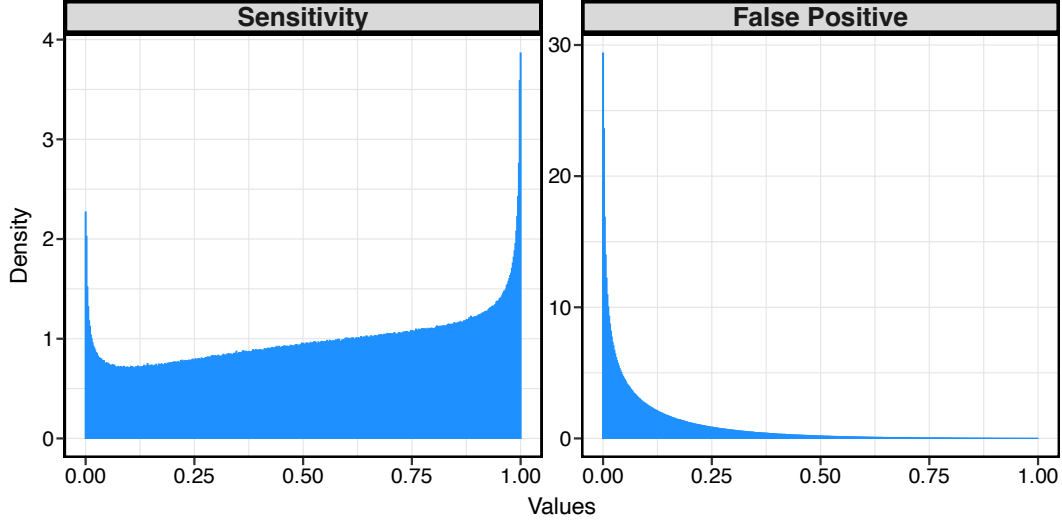


Figure S4: For 5 causes and default prior parameter choices mentioned in Section (S3), this is an example of prior on sensitivity (left panel) and false positive (right panel) in each country.

and *out-of-sample* performances in each country averaged over MITS-VA cause pairs. The top and middle panels assess average *mean square errors* of *posterior means* and average *interval scores* for the 95% *credible intervals*, evaluating the in-sample performance of point estimates and heterogeneity quantification (Gneiting and Raftery, 2007; Bosse et al., 2022). With the use of random effects (See (7) in the main article) in quantifying heterogeneity, the degree of heterogeneity is reflected by the uncertainty surrounding the homogeneous proportions (fixed effects). So, for analyzing the out-of-sample performance of heterogeneity prediction, we present average interval scores of 95% *prediction intervals* in the bottom panel. In summary, we find that all methods exhibit similar performance when the misclassification matrix is truly homogeneous. However, in situations where sensitivities exhibit heterogeneity, both of the heterogeneous methods perform similarly to each other, and they either surpass the performance of the homogeneous model or perform similarly to it. Finally, in cases where the misclassification matrix is fully-heterogeneous, the fully-heterogeneous method significantly outperforms both the homogeneous and partly-heterogeneous methods. This highlights the efficacy of the fully-heterogeneous method in flexibly adapting to different situations and demonstrating its superior performance in capturing and quantifying heterogeneity.

S5 Model Selection and Out-of-sample Performances in InSilicoVA’s Misclassification Analysis Based on CHAMPS

In Figure S7, we compare model selection performances of different methods in the case of neonatal deaths for InSilicoVA in CHAMPS. We calculate the *widely applicable information criterion* (WAIC) and *Leave-one-out cross-validation information criterion* (LOO-IC), two metrics commonly used in the literature. Compared to the homogeneous method, the partly-heterogeneous method enhances the information criteria by 6–7%. However, the fully-heterogeneous method outperforms all, improving the criteria by 5–8% over partly-heterogeneous and an impressive

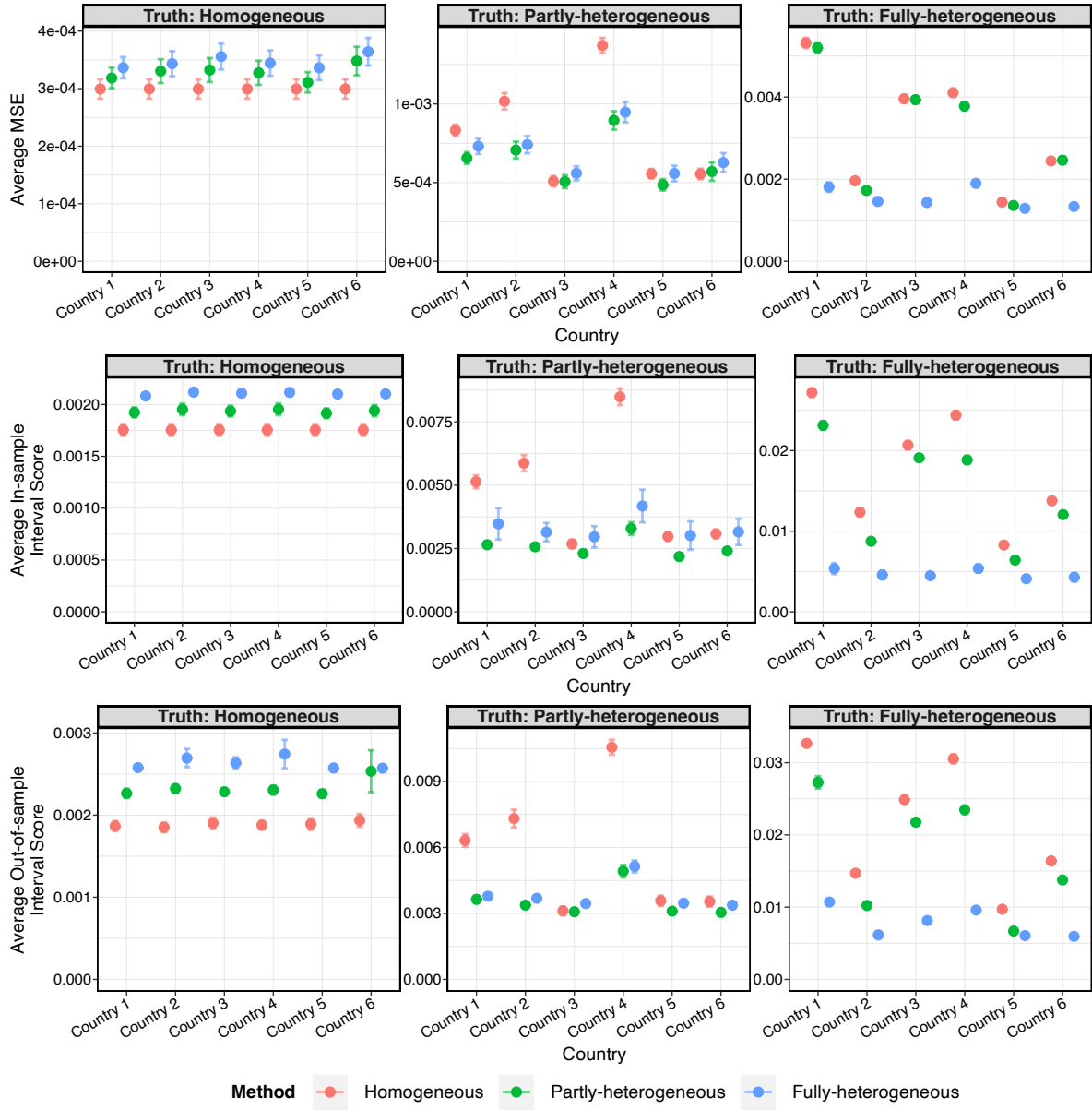


Figure S5: Averaged across all MITS-VA cause pairs over 50 replications, the figure compares in-sample mean squared errors of posterior means (top panel), in-sample interval scores of 95% credible intervals (middle panel), and out-of-sample interval scores of 95% prediction intervals (bottom panel) for all methods. Lower values are better. Columns show different true simulation scenarios. The error bars indicate ± 1 Monte-Carlo standard error.

11–15% over the homogeneous method. This highlights the efficacy of the fully-heterogeneous method in capturing and quantifying heterogeneity.

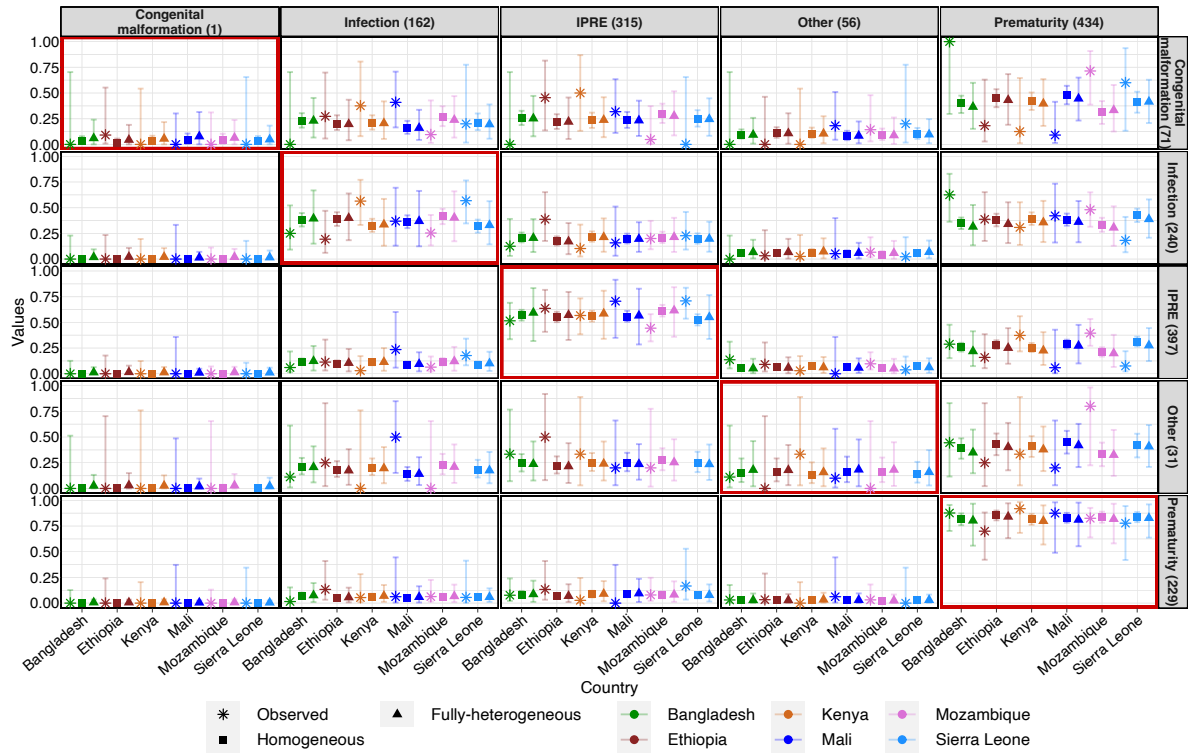


Figure S6: Comparison of observed misclassification rates with out-of-sample point (predictive mean) and uncertainty (95% prediction interval) predictions from homogeneous and fully-heterogeneous methods. Rows and columns refer to MITs and VA-predicted causes.

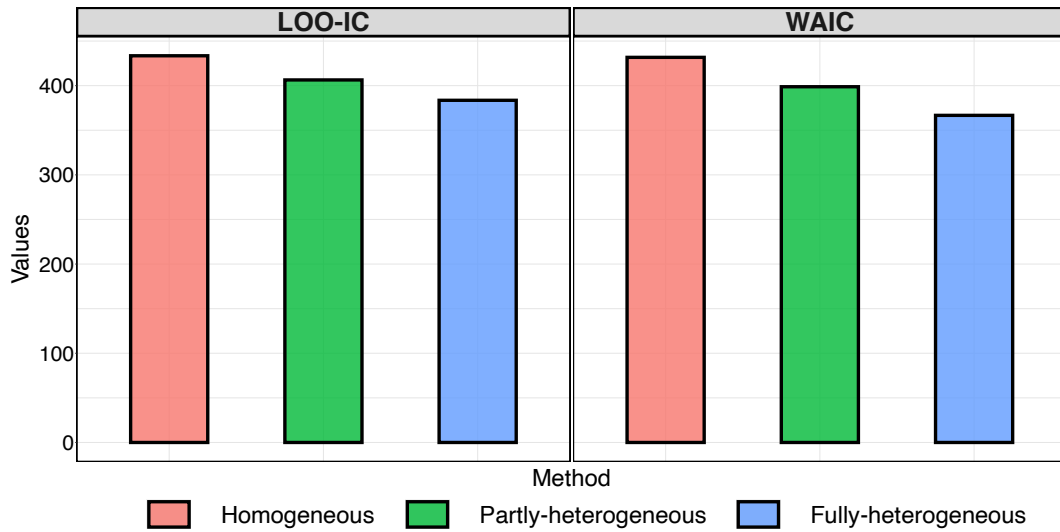


Figure S7: For neonatal deaths in CHAMPS for InSilicoVA, the bar plots compare widely applicable information criterion (WAIC) and Leave-one-out cross-validation information criterion (LOO-IC) from the three methods. Lower values are better.

References

- Bosse, N. I., Gruson, H., Cori, A., van Leeuwen, E., Funk, S., and Abbott, S. (2022). Evaluating forecasts with scoringutils in r. *arXiv*.
- Gneiting, T. and Raftery, A. E. (2007). Strictly proper scoring rules, prediction, and estimation. *Journal of the American Statistical Association*, 102(477):359–378.